

1 ***Application and comparison of different statistical methods for the***
2 ***analysis of groundwater levels over time: response to rainfall and***
3 ***resource evolution in the Piedmont Plain (NW Italy)***

4
5 ***Susanna Mancini¹, Elena Egidio¹, Domenico Antonio De Luca¹, Manuela Lasagna^{1*}***

6 ***¹University of Torino (Earth Sciences Department)***

7 ***Via Valperga Caluso 35, 10125 Torino (Italy)***

8 ****corresponding author: manuela.lasagna@unito.it***

9
10
11 **Abstract**

12 Monitoring and analysis of groundwater level (GWL) in space and time is one of the tools used
13 to evaluate the quantitative status of groundwater (GW) resources and identify possible
14 alterations and critical cases due to climate change and variability, anthropogenic influences
15 and other driving factors.

16 In this study, four statistical methodologies (trend, change-point, percentile and non-
17 standardized anomaly analyses) were applied for GWL and rainfall (R) analysis in the
18 Piedmont Plain (western Po Plain, NW Italy). To detect the interannual variations in the GW
19 maximum annual amplitude, the coefficient of variation was also used.

20 The aims of the study were 1) to compare the results of different statistical methods,
21 highlighting their applicability and differences to evaluate the quantitative evolution of GW,
22 2) to identify the relationship between GWL and R, 3) to investigate the spatiotemporal

23 variation in the GWL of shallow aquifers in the Piedmont Plain, and 4) to describe critical
24 situations of GW depletion.

25 The study highlights that the application of a single method for assessing the shallow GW
26 resource status does not always guarantee a reliable evaluation. For this reason, it is advisable
27 to apply different analysis methods at the same time. Completeness of data and medium to
28 long time series are prerequisites for meaningful analyses. The use of the same time interval
29 is always necessary for comparisons between different monitoring wells and between the
30 results of different statistical analyses. Last, by spatialising the results, it was possible to
31 identify areas characterised by similar GWL behaviour due to hydrological structure, climate
32 variability, land use and the evolution of anthropogenic activities over time. These factors
33 influence vary locally in the Piedmont plain and require local assessments to determine the
34 impact of changes in GWL.

35

36 Keywords: groundwater levels, rainfall, time series, statistical analysis, trends, change points,
37 anomalies, percentiles, interannual variations, Piedmont Plain

38 **Acronyms**

AN	Non-standardized anomalies
ChP_GWL	Change point in GWL time series
ChP_R	Change point in R time series
ChPA	Change point analysis
CV	Coefficient of variation
CV_GWL	Coefficient of variation of the maxima amplitude of annual GWL_range fluctuations
CV_R	Coefficient of variation of cumulative annual rainfall
GW	Groundwater
GWL	Groundwater level
GWL_range	Maximum amplitude of GWL annual fluctuations
GWL_AN	Groundwater level anomaly

GWL_max	The highest monthly mean GWL value
GWL_min	The lowest monthly mean GWL value
GWL_T	Groundwater level trend
PCTL	Percentiles analysis
R	Rainfall
R_AN	Rainfall anomaly
R_T	Rainfall trend
T	Trend analysis

39

40

1. INTRODUCTION

41

Groundwater (GW) constitutes the predominant reserve of fresh water on the planet and is

42

usually large and widely distributed in the world. Groundwater contributes 42%, 36% and 27%

43

of the water used for irrigation, households and manufacturing, respectively, during 1998-

44

2002 (Döll et al., 2012). In recent decades, GW depletion has been detected in different parts

45

of the world (Döll and Fiedler, 2008, Wada et al., 2010) due to increasing populations,

46

anthropic activities (e.g., overexploitation), and climate change (Taylor et al., 2013, Voss et

47

al., 2013, Wu et al., 2020). Increasing temperature and evapotranspiration, snow cover

48

retreat, and changing patterns and/or decreasing rainfall (R) and snow are among the major

49

consequences attributed to climate change, and they can negatively impact GW recharge

50

(IPPC, 2022).

51

The impacts of climate change on GW resources may be even more severe and amplified by

52

intensive groundwater extraction, that represents a secondary effect of climate change itself.

53

Climatic and anthropogenic factors are many, impact GW resources in different ways, often

54

overlap, and are difficult to separate (EEA, 2018). For this reason, many GW resource studies

55

separately analyse their effects (Taylor et al., 2013, Russo and Lall, 2017).

56

Long-term monitoring and analysis of groundwater level (GWL) showed to be important tools

57

for identifying possible alterations in the quantitative status and for highlighting the response

58 of GW to climate change and the other anthropogenic global change drivers (IAH, 2016,
59 Whittemore et al., 2016).

60 Statistical methods for the investigation of climatic parameters and hydrogeologically related
61 time series are many.

62 Trend analysis (T) has been extensively used to assess the potential impacts of climate change
63 and variability on natural and hydrological data, such as R, streamflow and GWL time series,
64 in various parts of the world (Hirsch et al., 1982, Zwilling et al.,1989, Serrano et al., 1999,
65 Zhang et al., 2001, Burn and Elnur, 2002, Arora et al., 2005, Birsan et al., 2005, Svensson et
66 al., 2005, Abdul Aziz and Burn, 2006, Polemio and Casarano, 2008, Stahl et al. 2010, Xu et al.,
67 2010, Zheng, et al., 2010, Liu et al., 2011, Panda et al. 2012, Rusi et al., 2013, Lutz A. et
68 al.,2015, Patle et al. 2015, Polemio, 2016, Amogne et al., 2018, Ducci and Polemio, 2018,
69 Kumar et al., 2018, Pathak and Dodamani, 2019, Xia et al., 2019, Bastiancich et al., 2021). The
70 nonparametric Mann-Kendall trend test (Mann, 1945, Kendall, 1955) and Sen's slope
71 estimator (Sen, 1968) were applied for analyzing trends of GWL and climatic variables in
72 different studies (Kawamura et al., 2011, Tabari et al., 2011, Krishan et al., 2015, Ribeiro et
73 al., 2015, Lasagna et al., 2019).

74 Indeed, nonparametric statistical tests do not require the data to follow a particular
75 distribution, and they are not very sensitive to the presence of possible outliers in the GWL
76 data, compared to the parametric ones (Caloiero et al., 2011).

77 However, statistical analyses on time series can provide different results depending on the
78 time period analyzed (Tomé and Miranda, 2004). Change point analysis (ChPA) can help
79 identify abrupt changes (change points) in a time series and then split the time series into
80 subperiods in which the parameters show homogeneous behaviours. The ChPA has been used
81 in the field of meteorology for the analysis of changes in climate data (Lanzante, 1996,

82 Beaulieu et al., 2012, Tirogo et al., 2016), such as air temperature, seasonal R (e.g., Tomozeiu
83 et al., 2000, Reeves et al., 2007, Lasagna et al., 2020a), precipitation and streamflow (Kiley,
84 1999, Xiong and Guo, 1994), temperature (Toreti et al., 2010) and carbon dioxide
85 concentration (Costa et al., 2016).

86 Other statistical analyses of fluctuations in GWL are based on the comparison of recent data
87 with a reference value (usually a mean level) or with a range of reference oscillations (usually
88 defined between the first and third quartile). In these cases, the considered reference values
89 can vary the magnitude of the results (Helsel et al., 2020).

90 The Percentiles Method (PCTL), applied to GWL time series, is a standard groundwater
91 evaluation tool used by the U.S. Geological Survey and proposed by the Ontario Ministry of
92 Environment (MOE, 2008). PCTL was considered an integration of the GW drought indicator
93 (Post, 2013). The 10th, 25th, 75th, and 90th percentiles were used to classify levels from much
94 below normal to much above normal; in general, GWL between the 25th and 75th percentiles
95 was considered normal, GWL between the 10th and 25th percentiles was considered dry, and
96 GWL below the 10th or 5th percentile was considered a drought emergency.

97 The evaluation of standardized and non-standardized anomalies are methods widely used for
98 the analysis of climatic variables such as R, air temperature and snowfall (Regione Piemonte,
99 2020, Asoka et al., 2017).

100 Analysis of seasonality, maximum annual amplitude of fluctuations, and interannual
101 variability of GWL also provide additional insight into natural (e.g., climate change/variability)
102 and anthropic (e.g., changes in irrigation practices) factors influencing the trend in GWL
103 (Lasagna et al., 2020b). Fluctuation in the GWL occurs due to numerous factors, such as
104 recharge (net recharge and discharge), evapotranspiration and withdrawal from wells. Its

105 magnitude also depends on climatic factors, drainage, topography, geological and
106 hydrogeological characteristics and anthropogenic influences (Panda et al., 2007, Krogulec et
107 al., 2020). Sometimes high fluctuations can result in problems and undesirable effects, such
108 as the alteration of GW flow regimes and changes in the volume and quality of available GW
109 resources (Apaydin, 2009). Indeed, a high variability of annual average GWL fluctuations over
110 time can lead to critical issues, such as, in the case of shallow aquifers, interference with
111 anthropogenic infrastructures or an incorrect assessment of the GW resource, which cannot
112 be detected through a single annual average value.

113 In this study, different statistical methodologies were applied for GWL and rainfall (R) analysis
114 in the Piedmont Plain (western Po Plain, NW Italy).

115 A preliminary study of the hydrodynamic behaviours of the GW, their spatial distribution and
116 R regime was conducted in this area by Lasagna et al. (2020b). Moreover, the main change
117 drivers, especially those created by land use and climate variability in the study area, were
118 analyzed and described.

119 This study represents a continuation and a deepening of Lasagna et al.'s (2020b) investigation.
120 Starting from the current resource status, it aims to describe the most useful methods to
121 investigate critical situations of GW depletion due to climate variability, land use and human
122 activities. More specifically, four methods of GWL time series analysis were applied and
123 compared: trend, change-point, percentile and non-standardized anomaly analysis. The same
124 methodologies were applied to the R and GWL time series. Although changes in GW levels do
125 not depend solely on climate data, comparisons and correlations between GWL and R can
126 help to assess aquifer vulnerability to climate change (Ng et al., 2010) and to evaluate how R
127 affects changes in the GWL. The aims of the study were: 1) to compare the results of different
128 statistical methods, highlighting their applicability and differences; 2) to identify the

129 relationship between GWL and R; 3) to investigate the spatiotemporal variation in the GWL
130 of shallow aquifers in the Piedmont Plain; and 4) to describe critical situations of GW
131 depletion. Then, the spatialization of the results of the statistical analyses and elaborations
132 were discussed, with particular reference to geographical distribution, identifying the most
133 critical areas .

134

135 **2. MATERIALS AND METHODS**

136 **2.1 The study area**

137 The study area is the Piedmont Plain (western Po Plain, NW Italy) and represents the largest
138 and most important GW resources in the Piedmont Region.

139 The Piedmont Plain is characterized by different hydrogeological complexes (Fig. 1) listed
140 from top to bottom (Bove et al., 2005, De Luca et al., 2019, Perotti et al. 2019, De Luca et al.,
141 2020) as follows:

- 142 • Recent fluvial deposits (Upper Pleistocene-Holocene): composed of incoherent and
143 heterometric sediments of fluvial (Holocene) and fluvioglacial (Upper Pleistocene) origin,
144 mainly composed of gravel and sand with subordinate silty-clay intercalations; these
145 sediments are located in the bottom of the valleys of the region and in the Piedmont Plain.
- 146 • Medio-ancient fluvial deposits (Middle-Lower Pleistocene): composed of incoherent
147 and heterometric sediments, locally cemented, mainly gravel and sand, and silty-clay,
148 sometimes in alternation; the fine fraction may be prevalent. These deposits, which border
149 the Apennine-Alps chains from Tanaro River to Maggiore Lake, are in contact with the
150 morainic arches to which they are genetically connected.

151 • Glacial deposits and morainic hills (Pleistocene): constituted by heterogenic glacial
152 deposits as silt and clay with sand, cobbles and boulders.

153 • Lacustrine, swamp and fluvial sediments (Villafranchian series) (Upper Pliocene-
154 Lower Pleistocene): fluvial-lacustrine deposits characterized by alternations of silty-clayey
155 and gravelly sandy horizons.

156 • Marine sand and clayey silt (Pliocene): marine sediments that constitute the
157 substratum of the Villafranchian series.

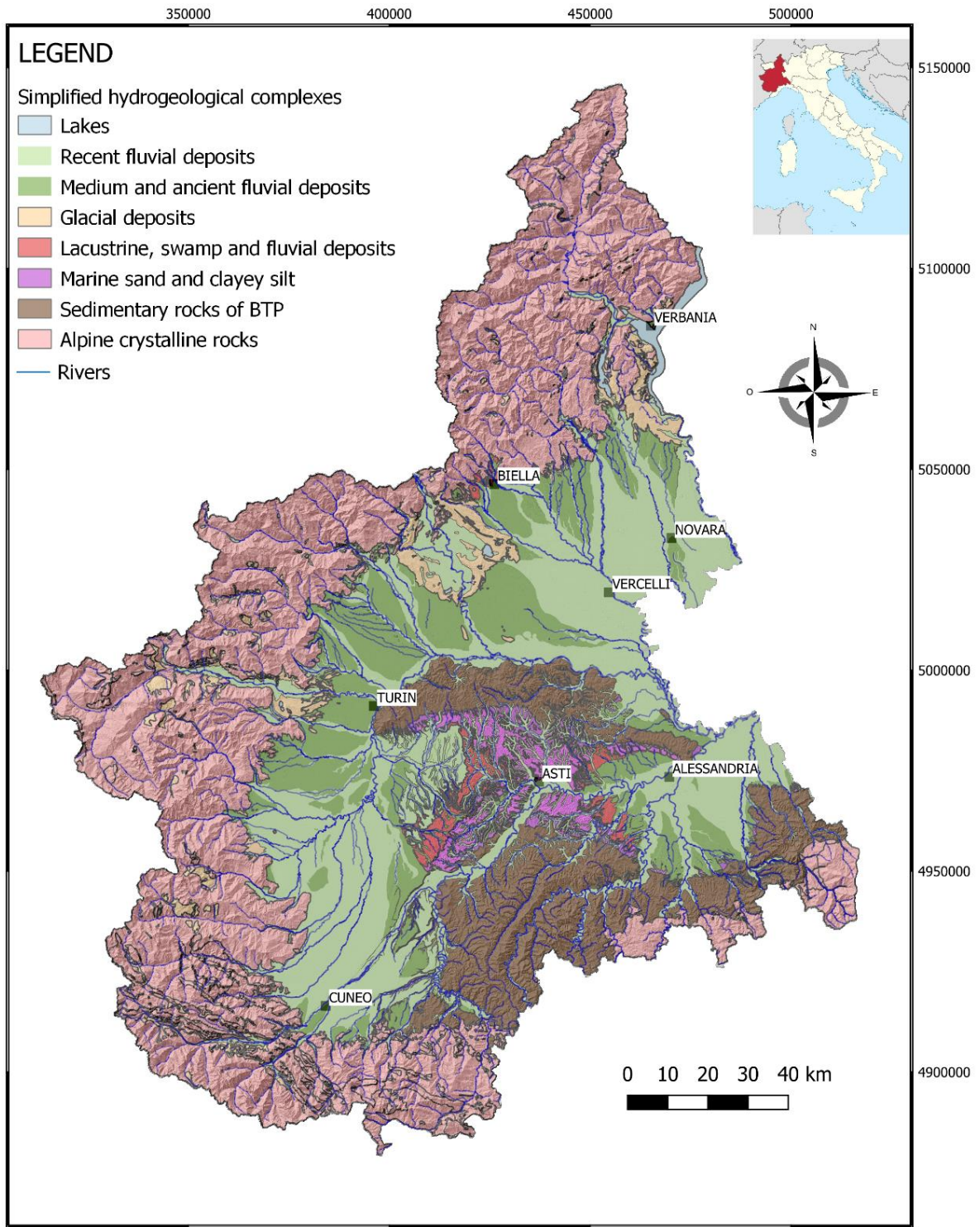
158 The Piedmont Plain is surrounded by the crystalline bedrocks (magmatic and metamorphic
159 rocks) of the Alps to the N and W and by Tertiary Piedmont Basin (BTP) Hills (pre-Pliocene
160 marine sediments characterized by conglomerate, sandy arenaceous formations and
161 evaporitic deposits) to the S and E. A more detailed description of the geological setting with
162 simplified cross sections can be found in De Luca et al. (2020) and in Lasagna et al. (2020b).

163 The shallow unconfined aquifer is hosted in the Quaternary alluvial deposits complex (Middle-
164 Lower Pleistocene-Holocene). This complex has a thickness generally ranging between 20 and
165 50 m, and the hydraulic conductivity varies from high values ($K > 10^{-3}$ m/s) of recent fluvial
166 deposits to medium ($K = 10^{-5} - 10^{-3}$ m/s) and low values ($K = 10^{-7} - 10^{-5}$ m/s) of medium-
167 ancient fluvial deposits. The lower hydraulic conductivity is characteristic especially of the
168 oldest and altered levels.

169 The water table depths from the ground surface are in large areas less than 5 m, for example,
170 in the northern sector of the Piedmont plain (Vercelli and Novara plains), in the areas along
171 the main watercourses (Po and Tanaro rivers) and in the plain between Turin and Cuneo.
172 Along the band of the foothills and in particular west of Turin and southwest of Cuneo, the
173 water table is deeper, with values generally more than 15-20 m from the ground surface. The
174 highest values (more than 40 m) are distributed in the Cuneo Plain and in the northern part

175 of the Turin Plain due to the presence of a high morphological terrace. In the south-eastern
176 part of the Piedmont Plain (Alessandria Plain), the water table depths vary between 5 and 15
177 m from the ground surface (De Luca et al., 2020). Deep aquifers are located in the
178 Villafranchian series and in the sandy facies of the Pliocene marine complex (Lasagna et al.,
179 2014, Castagna et al., 2015).

180 In this paper, GWL analysis is conducted in an unconfined shallow aquifer characterized by
181 medium-high hydraulic conductivity. Recharge areas of the unconfined aquifer are mainly due
182 to infiltration of R and infiltration from the river leakage from the loosing streams in the high
183 plain sectors. The low plain sectors are generally discharge areas, and the Po River represents
184 the main regional discharge axis for the GW flow (Lasagna et al., 2018).



185

186 **Fig. 1.** Simplified hydrogeological map of the Piedmont region (NW Italy) (modified from
 187 Regione Piemonte, 2021b). Reference system: EPSG:32632 - WGS84/UTM zone 32N.

188

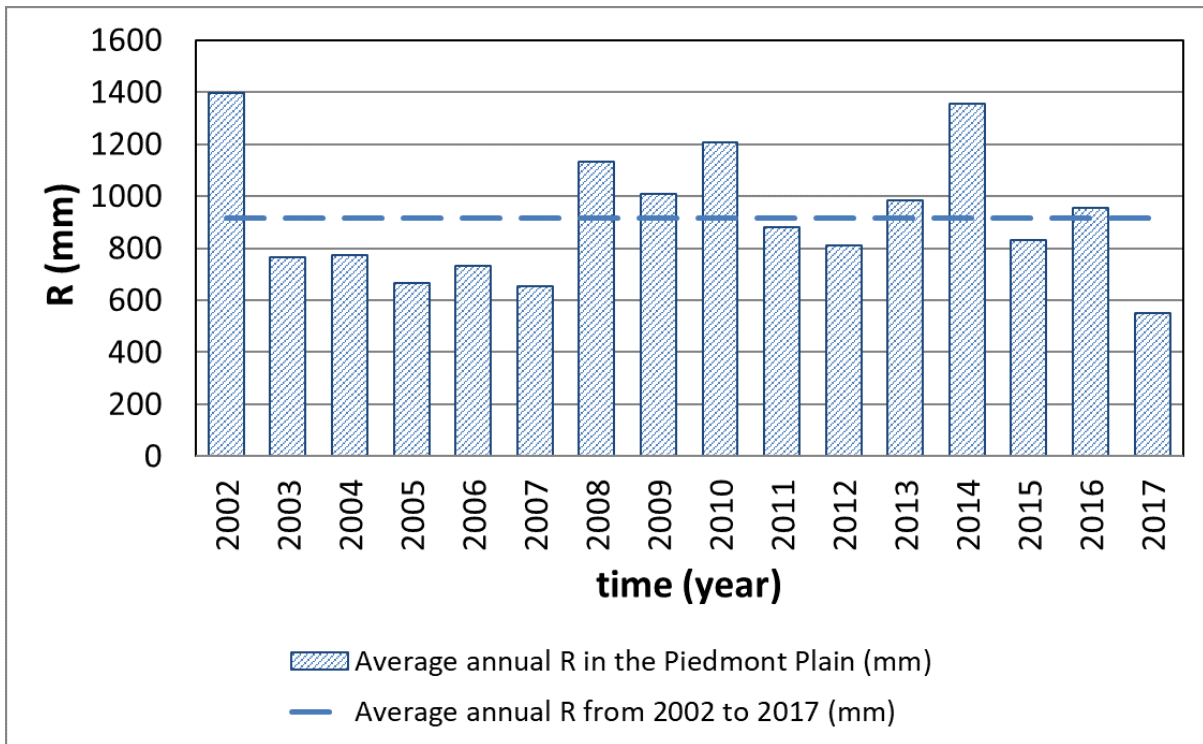
189 The physiographic configuration of the Piedmont region, surrounded on three sides by
190 mountain chains and hills, favours local circulations and microclimates. The climate
191 classification of the Piedmont Plain identifies a relatively arid central-southern area (plain of
192 Asti and Alessandria) surrounded by a more humid area (Biancotti et al., 1998).

193 The analysis of the annual average temperature anomalies in the Piedmont, calculated for the
194 period 1958-2015, shows an increasing trend over the past twenty years, with an estimated
195 total increase of approximately 1.2 °C over 50 years (ARPA, 2010). The years after 1985 show
196 a more marked increase in average temperature, and the increase is mainly concentrated in
197 the winter, spring and summer months.

198 The average annual R from 2002 to 2017 in the Piedmont Plain was over 900 mm. During that
199 period, 2002 was the wettest year, and 2017 was the driest (Fig. 2). The average annual R
200 showed the lowest values (less than 750 mm/yr) in the SE part of the Piedmont Plain (Asti and
201 Alessandria plain), medium values between 750 and 900 mm/yr in the central part (Cuneo
202 and southern Turin Plains), and the highest values between 750 and 1200 mm/yr in the
203 northern part (Novara, Vercelli and Biella Plains) (Fig. 3). The highest values of annual R were
204 detected along the border of Plain with the mountain relief (> 900 mm/yr). These values
205 showed a similar spatial distribution detected for the period 1959-2009 (ARPA, 2010).

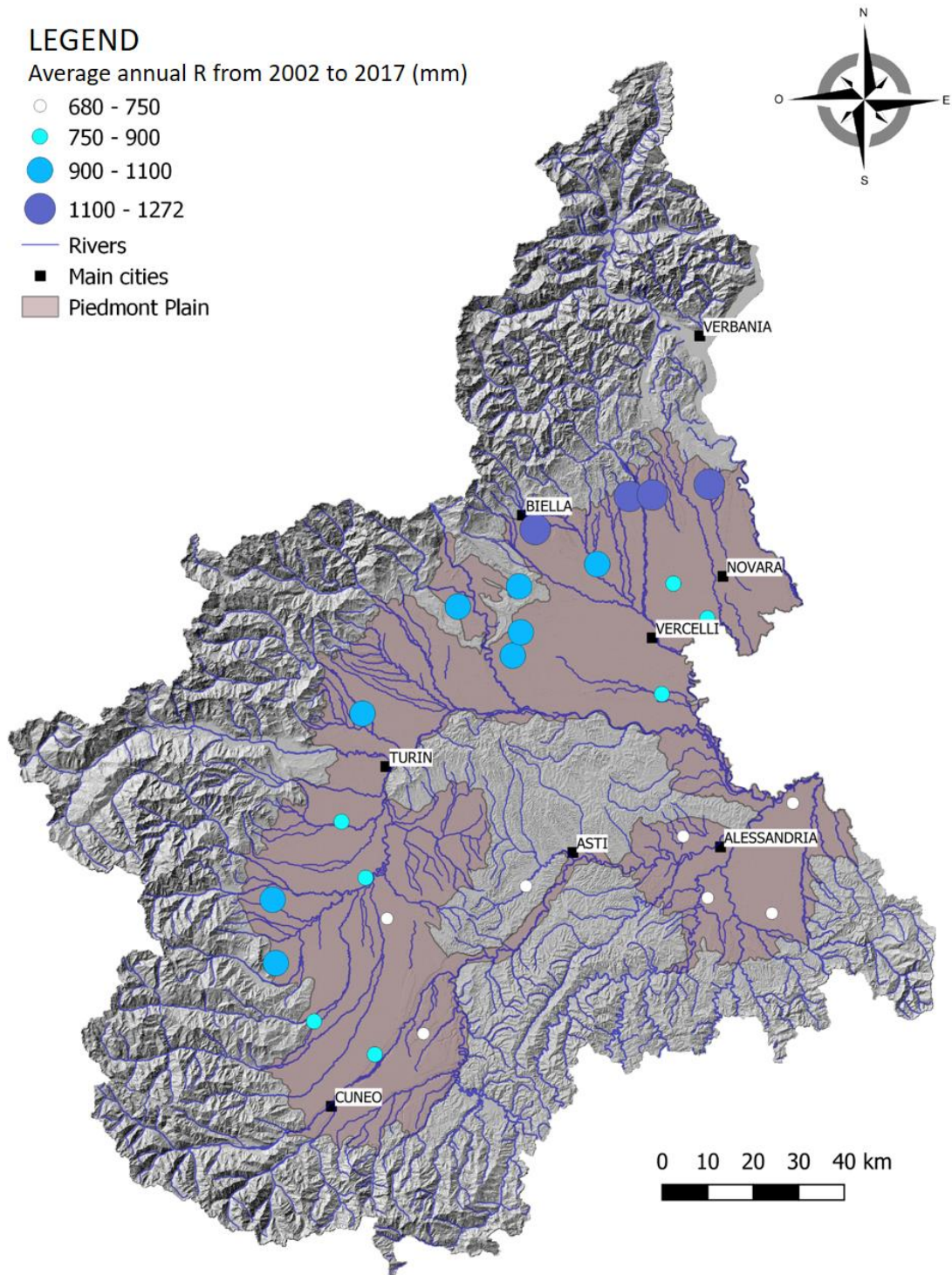
206 The annual R in the Piedmont Plain showed a seasonal behaviour characterised with a
207 bimodal trend, with 2 maxima (spring and autumn) and 2 minima (winter and summer) typical
208 of a continental climate (prealpine or subalpine) (Acquaotta and Fratianni, 2013, Baronetti et
209 al., 2018).

210



212

213 **Fig. 2.** Average annual R of rain gauges analyzed in the Piedmont Plain (light blue dashed
 214 line: the average annual R from 2002 to 2017).



215

216 **Fig. 3.** *Spatial distribution of annual R (average 2002-2017) in the Piedmont Plain.*

217 Regarding snowfall in the Piedmont Mountains, Acquavotta et al. (2013) evaluated the annual
218 cumulative average snowfall of the reference period 1961-2010, recorded at altitudes higher
219 than 1000 m, varying from a minimum of approximately 300 cm to a maximum of 700 cm.
220 2008 was the year in which snowfall was highest, after 1950, in the last 30 years (ARPA, 2016).

221

222 **2.2 Methods**

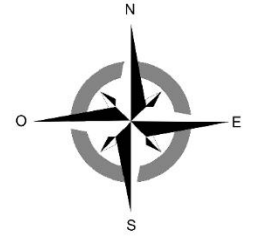
223 **2.2.1 Monitoring network and data analysis**

224 For this study, the GWL of the shallow aquifer in 36 monitoring wells and the daily R data from
225 26 rain gauges distributed in the same area were analyzed (Fig. 5). The monitoring wells,
226 homogeneously distributed in the Piedmont plain, are part of the automatic monitoring
227 network of the Regional Agency for the Protection of the Environment (ARPA), which has
228 been activated since 2000. Daily GWL data are available on the website of the Regione
229 Piemonte (Regione Piemonte, 2021b).

230 R data are part of the automatic monitoring network Agrometeorological network (RAM)
231 managed by Regione Piemonte, which has been activated since 2000. The R data are available
232 on the RAM website (Regione Piemonte, 2021c).

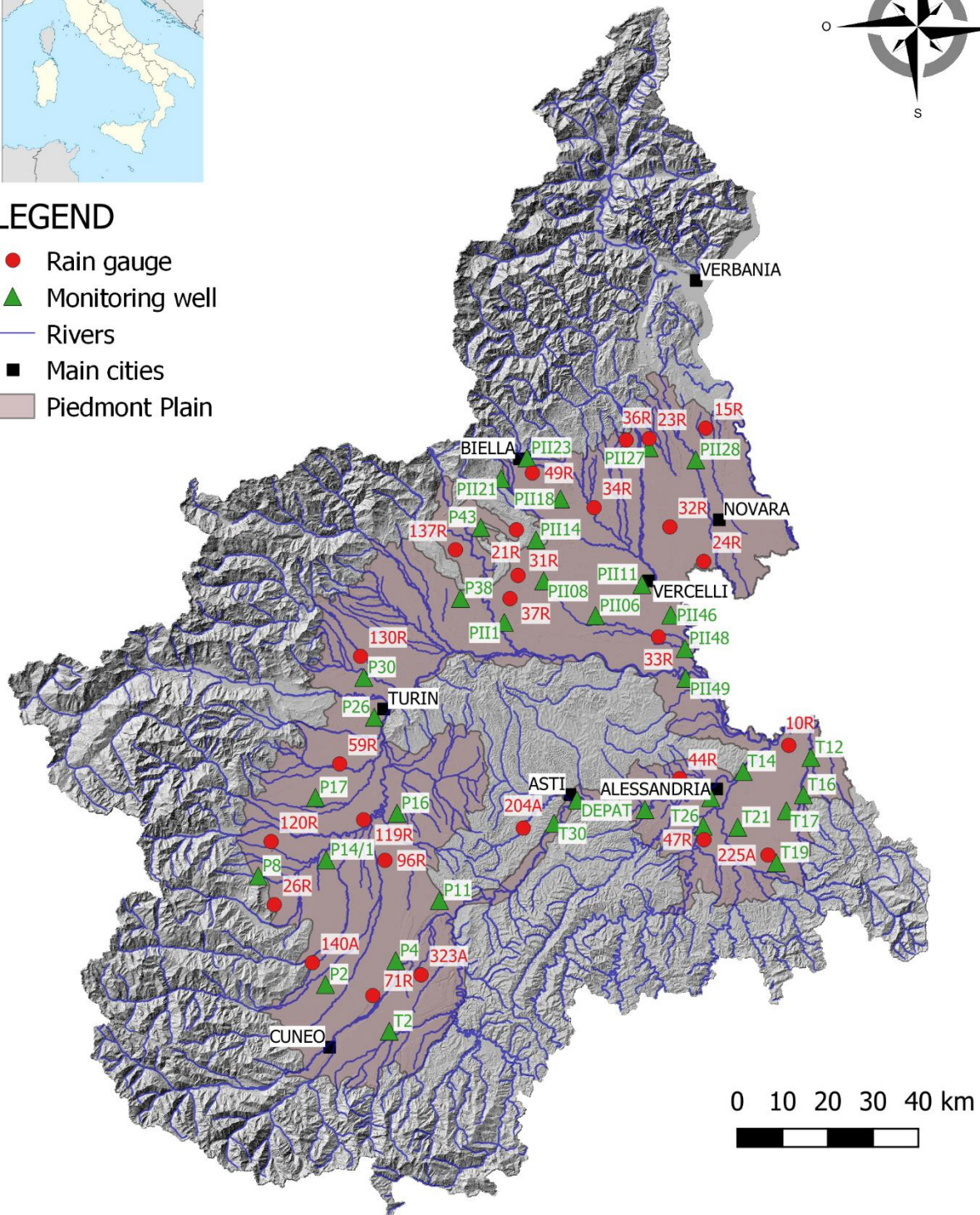
233 The analysis of GWL and R time series was carried out considering a standard period of 16
234 years between 1 January 2002 and 31 December 2017. In this period, all the analyzed time
235 series showed a low percentage of missing data (completeness of more than 90% for GWL
236 data and 100% for R data). Further information about GWL and R time series are reported in
237 Lasagna et al. (2020b).

238 Data were aggregated monthly, obtaining monthly averages of GWL and cumulative monthly
239 R. Moreover, GWL was also aggregated annually.



LEGEND

- Rain gauge
- ▲ Monitoring well
- Rivers
- Main cities
- Piedmont Plain



240

241 **Fig. 4.** Monitoring wells and rain gauges used for the study in the Piedmont Plain.

242 **2.2.2 Data analysis**

243 The first elaboration in this study aimed to identify the following:

- 244 • the maximum amplitude of the GWL annual fluctuation and the average in the period
245 2002-2017 to quantify the annual variation in the water table in each monitoring well;
- 246 • the interannual variability in the maximum amplitude of GWL fluctuations
247 (GWL_range) for each monitoring well in the analyzed period to distinguish wells that
248 present a constant amplitude of fluctuation over time from those characterized by
249 higher variability. These elaborations were conducted determining the coefficient of
250 variation CV of annual maximum amplitude of GWL fluctuation (CV_GWL).

251 These parameters and their spatialisation permitted to identify the areas that contain the
252 greatest annual fluctuations and/or high interannual variability.

253 Different statistical methods were applied to the GWL and R time series, including a) change-
254 point analysis (ChPA); b) trend analysis (T); c) percentile method (PCTL); and d) analysis of the
255 non-standardized anomalies (AN). The elaborations of trends, change-points, and percentiles
256 were performed using monthly data. Regarding the non-standardized anomalies, the analysis
257 was performed on monthly and annually aggregated data.

258 Finally, comparisons were made between interannual variations, trends, change points and
259 anomalies evaluated for R and those evaluated for GWL.

260 In the following, a detailed description of each adopted methodology is reported.

261

262 **2.2.2.1 Interannual variability and amplitude of average annual GWL fluctuations**

263 An accurate estimation of the spatial and temporal fluctuations in GWL and recharge is
264 important in the management of GW resources (Rai and Singh., 1985, Cuthbert et al., 2015).

265 For each monitoring well, the maximum amplitude of GWL annual fluctuations (GWL_range)
266 was evaluated in the period 2002-2017. The GWL_range was calculated for each year as the
267 difference between the highest monthly mean GWL value (GWL_max) and the lowest
268 monthly mean GWL value (GWL_min) (Fig. S1, in supplementary materials). The maximum
269 amplitude of annual fluctuation in GWL can vary from year to year, so for each GWL time
270 series, the minimum and maximum values of annual GWL_range fluctuations were detected
271 (Fig. S2, in supplementary materials) in the analyzed period.

272 The interannual variation of annual GWL_range fluctuations were made through the
273 coefficient of variation (CV). The CV is independent of both unit and order of magnitude, and
274 is defined as the dispersion (standard deviation, σ) normalized by the mean (μ) and is
275 therefore a pure number (Soliani, 2001):

$$276 \quad CV = \frac{\sigma}{\mu} \quad (1)$$

277 The interannual variability in the maximum amplitude of annual GWL_range fluctuations
278 (CV_GWL) was evaluated in each monitoring well. The CV was also computed to evaluate the
279 interannual variations in the cumulative annual R (CV_R) and compared with the CV_GWL.

280 Finally, the average GWL_range values, CV_GWL and CV_R were plotted on a map to evaluate
281 their spatial distribution and the magnitude of their variability over time.

282

283 **2.2.2.2 Change-point analysis**

284 ChPA is a statistical tool for the identification of sudden changes (change points) in a time
285 series, determining whether and when a change has taken place.

286 In this study, ChPA was applied to search for potential significant changes in the monthly GWL
287 (ChP_GWL) and cumulative monthly R time series (ChP_R).

288 The analysis was performed by ordering the data according to time; then, the data were
289 tested by the statistical nonparametric Pettitt test (Pettitt, 1979).

290 The Pettitt test is based on the values assumed by the following statistics:

291

$$292 \quad U_{t,T} = \sum_{i=1}^t \sum_{j=t+1}^T \text{sgn}(X_i - X_j) \quad t = 1 \dots T \quad (2)$$

293

294 where T is the number of data in the series, X_i and X_j are data values at times i and j (with j >
295 i), respectively, and $\text{sgn}(X_i - X_j)$ is the sign function. For each value of t (instant of the series),
296 a value of U (t, T) is obtained and plotted. The analysis of the graph of the function U (t, T)
297 allows the identification of the moment at which a change point may have occurred. The
298 maximum or minimum point of the function U (t, T) represents the instant in which a change
299 point occurs if the outcome of the test were such that the null Hypothesis H_0 was rejectable
300 at the level of significance assigned.

301 For this study, a 95% confidence interval was required to state that the change was significant,
302 with a level of significance α of 0.05.

303 The research and the identification of change points allowed us to obtain complementary
304 information that could help to deepen the analysis of time series and their variability over
305 time and the variability of all other components directly or indirectly connected (Lockwood,
306 2001).

307 A change point in a GWL time series (ChP_GWL) corresponds to a shift in the local recharge
308 and discharge of the aquifer due to a combination of factors that can be natural (e.g., R,

309 feeding from watercourses, snow melt, evapotranspiration due to the rise in temperature) or
 310 anthropic (e.g., massive irrigation and paddy fields, and increase/decrease in water
 311 withdrawals during the year). The characteristics of the porous media that host the aquifer
 312 can influence the delay of the response time. The ChPA was applied over the whole time
 313 series 2002-2017, and the most important ChPs for both GWL and R were identified.

314 Purposes of the ChPA in this work were a) to detect if there is any change in the sequence of
 315 observed time series and when it occurred; b) to estimate the number of changes and their
 316 corresponding locations in time; c) to identify the points (moments) in which to start or end
 317 the trend (Fig.S3 and Fig. S4, in supplementary materials) and to compare the temporal
 318 location of ChP_GWL with the ChP_R and determine the magnitude of delays (in months).
 319 The ChPA preceded the trend analysis to split the time series into subperiods in which the
 320 parameters show homogeneous behaviours.

321 The ChPA was performed using the ANABASI tool version 1.51 beta, a statistical program
 322 developed by ISPRA (Braca et al., 2013).

323 **2.2.2.3 Trend analysis**

324 In this study, the nonparametric Mann-Kendall test was employed to identify statistically
 325 significant positive or negative monotonic trends in the GWL (GWL_T) and R (R_T) time series,
 326 and Theil-Sen's slope estimator allowed us to evaluate the magnitude of the trends.

327 The Mann-Kendall test statistic (S) was calculated according to:

$$328 \quad S = \sum_{k=1}^{n-1} \sum_{j=k+1}^n \text{sgn}(X_j - X_k) \quad t = 1 \dots T \quad (3)$$

$$329 \quad \text{with} \quad \text{sgn}(X) = \begin{cases} 1 & \text{if } X > 0 \\ 0 & \text{if } X = 0 \\ -1 & \text{if } X < 0 \end{cases} \quad \text{and} \quad X = X_j - X_k$$

330 A positive value of S is an indicator of an increasing trend, and a very low negative value
331 indicates a decreasing trend. For the Mann-Kendall test, when the null Hypothesis H_0 is
332 rejected at the level of significance α (0.05), the data present a statistically significant trend.

333 If a linear trend was present in a time series, Sen's slope estimator (Q_i) was used to estimate
334 the slope (magnitude of the trend line (i.e., rate of water level decline, m/yr):

$$335 \quad Q_i = \frac{X_j - X_k}{j - k} \quad \text{for } i = 1, 2, 3, \dots, N \quad (4)$$

336 where X_j and X_k are data values at times j and k (with $j > k$), respectively. T was conducted
337 defining a 5% significance level, and trends were assumed to be real for p values less than this
338 threshold ($p \text{ value} \leq 0.05$). The trend analysis was performed using the software ProUcl (EPA,
339 2016).

340 T was performed on the whole period between 2002 and 2017 and on two subperiods
341 identified by the presence of a main change point in the GW and R time series. Studies applied
342 to climate variables (Tomé and Miranda, 2004) have shown a calculation of the total linear
343 trend as the weighted average of the partial linear trends with the identified change points
344 as boundaries.

345 GWL_T and R_T were then elaborated on the entire period of the time series (2002-2017) and
346 in shorter periods (2002-2008 and 2009-2017), delimited by the presence of a main change
347 point in the year 2008 (Fig. S3 and Fig. S4, in supplementary materials). Finally, the spatial
348 distributions of the GWL and R trends were mapped.

349 **2.2.2.4 Percentiles method**

350 PCTL allowed us to identify, for each measurement station, a threshold limit of GWL below
351 which the GW resource starts to show issues.

352 The PCTL method, proposed by ISPRA (ISPRA, 2017), is based on the measure of the “natural
353 fluctuation band” obtained by interpolating the monthly values of the 25th and 75th
354 percentiles computed in the time interval 2002-2015 (Fig. S5, in supplementary materials).
355 GWL below the range of natural oscillation of GWL (less than 25th percentile) places the
356 aquifer body in a condition of ‘Alert’ from the point of view of the quantitative status. Values
357 of GWL below 15-30% of the natural annual oscillation band are considered critical conditions
358 for the quantitative status of water body monitoring.

359 In this study, threshold values were set to 15% of the natural fluctuation band below the 25th
360 percentile of GWL (GWL_threshold of Fig. S5, in supplementary materials).

361 Finally, a spatial distribution of the number of months (for the year 2017 as an example of the
362 method application) below or above the defined threshold was performed.

363

364 **2.2.2.5 Non-standardized Anomalies**

365 A climatic anomaly is calculated from the difference between the annual (or monthly) values
366 (X) of the hydrological variable (e.g., R) and the average values of the reference period (μX_{ref})
367 of the hydrological variable considered:

$$368 \quad AN = X - \mu x_{ref} \quad (5)$$

369 According to the World Meteorological Organization (WMO, 2017), the reference period to
370 detect the level of anomaly of the analyzed variable should be at least 30 years (i.e., 1961-
371 1990, 1991-2020). However, it was found that 10–12 years of data provided a predictive skill
372 similar to that from a standard 30-year period. While such short periods cannot be considered
373 to be climatological typical standards or references, they are still useful to many users, and in
374 many cases, there will be benefits to calculate such averages operationally (WMO, 2007).

375 The non-standardized anomaly (AN) method was applied to the annual GWL and R data. The
376 reference values (GWL_{ref} and R_{ref}) were computed considering the average values of the
377 period 2002-2015. (Fig. S6, in supplementary materials).

378 A negative anomaly indicates that the observed GWL was lower than the reference value,
379 while a positive anomaly indicates that the observed GWL was higher than the reference
380 value. Finally, a spatial distribution of the positive and negative annual anomaly values for
381 2017 was performed.

382 **3. Results**

383 **3.1 Interannual variability and amplitude of average annual GWL fluctuations**

384 From 2002-2017, the average GWL_{range} fluctuations in the Piedmont Plain varied between
385 0.37 m (monitoring well PII21) and 4.58 m (T17) (Table 1 in supplementary materials). The
386 minimum annual GWL_{range} fluctuation was 0.19 m (P43 in 2007), whereas the maximum
387 value was 7.48 m (T17 in 2015).

388 Most of the monitoring wells showed an average of the maximum amplitude of GWL annual
389 fluctuations lower than 2 m. More specifically, 36% of the monitoring wells had an average
390 GWL_{range} lower than 1 m, and 44% had an average GWL_{range} between 1 and 2 m. Only
391 11% of the monitoring wells showed an average GWL_{range} between 2 and 3 m, and the
392 remaining 9% had values higher than 3 m (Fig. 5).

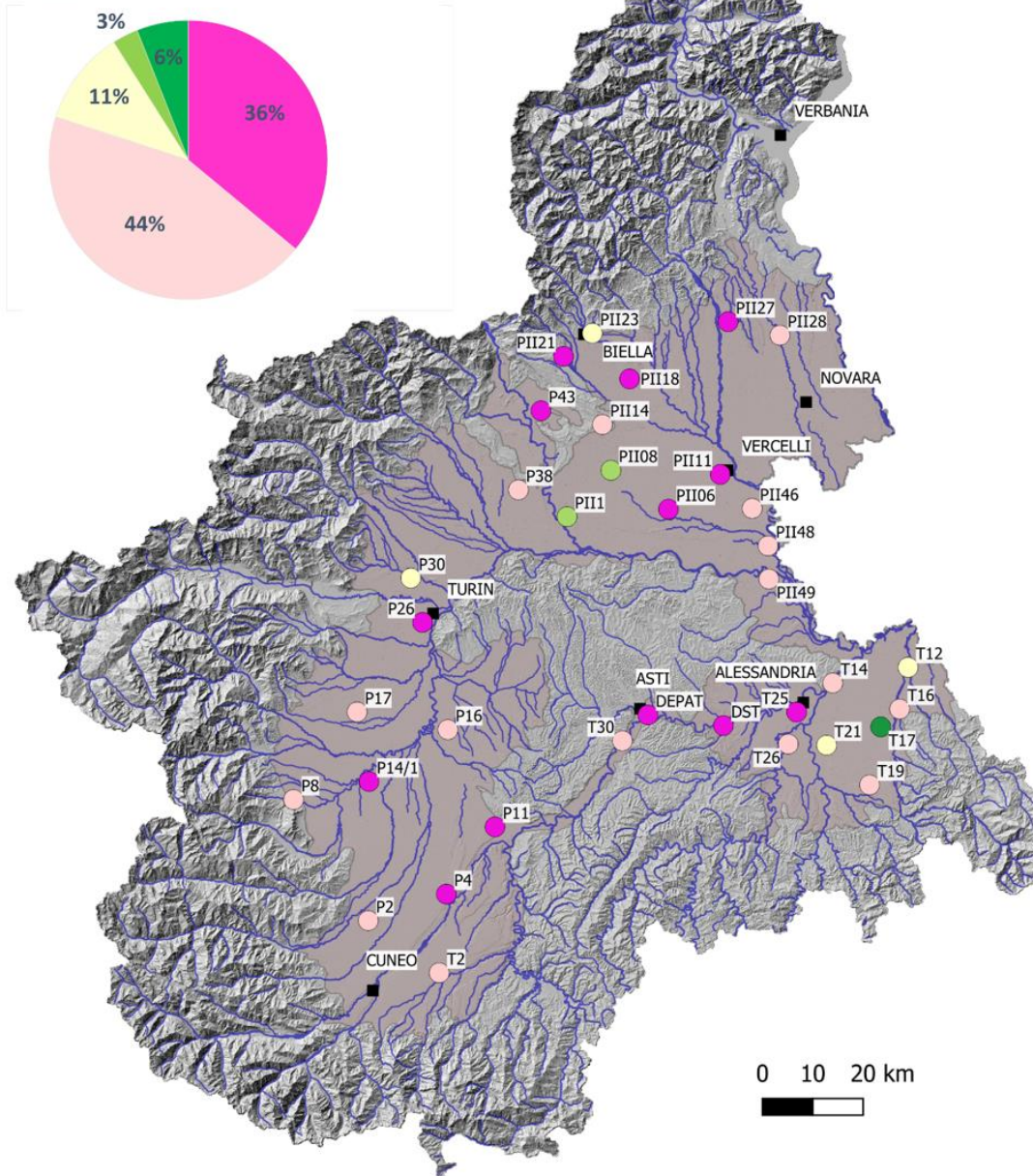
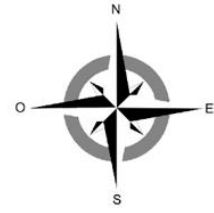
393 Monitoring wells located in the Cuneo Plain, in the southern part of the Turin Plain and at the
394 base of the mountain reliefs showed an average GWL_{range} lower than 2 m. Average
395 GWL_{range} values higher than 2 m were found in monitoring wells located in the Alessandria
396 Plain and along the western edge of the paddy field area in the Vercelli Plain.

LEGEND

Average 2002-2017 of annual GWL_range

- < 1 m
- 1 - 2 m
- 2 - 3 m
- 3 - 4 m
- > 4 m

- Main cities
- Rivers
- ▭ Piedmont plain area



397

398 **Fig. 5.** Spatial distribution of average 2002-2017 of annual GWL_range fluctuations

399 The CV allowed us to measure the relative variability of interannual GWL_ranges and thus to
400 compare groups of data according to their degree of variability. In the study area, the CV of
401 the annual GWL_ranges (CV_GWL), evaluated for each GW time series, varied from a
402 minimum of 0.11 to a maximum of 0.47. The CV_GWL allows separating the GWL time series
403 into 3 different groups (Table 1, in supplementary materials).

404 The highest interannual variations in the GWL (observed in 25% of the total wells) were
405 located in the Alessandria Plain (CV_GWL > 0.40). The lowest variations (22% of the total
406 wells) were located in the paddy field area (Vercelli and Novara plains CV_GWL <0.20). In the
407 other areas of the Piedmont plain (the remaining 53% of wells), the CV has intermediate
408 values ($0.20 < CV_GWL < 0.40$) (Fig. 6).

LEGEND

CV of annual GWL_range

- < 0.20
- 0.20 – 0.40
- > 0.40

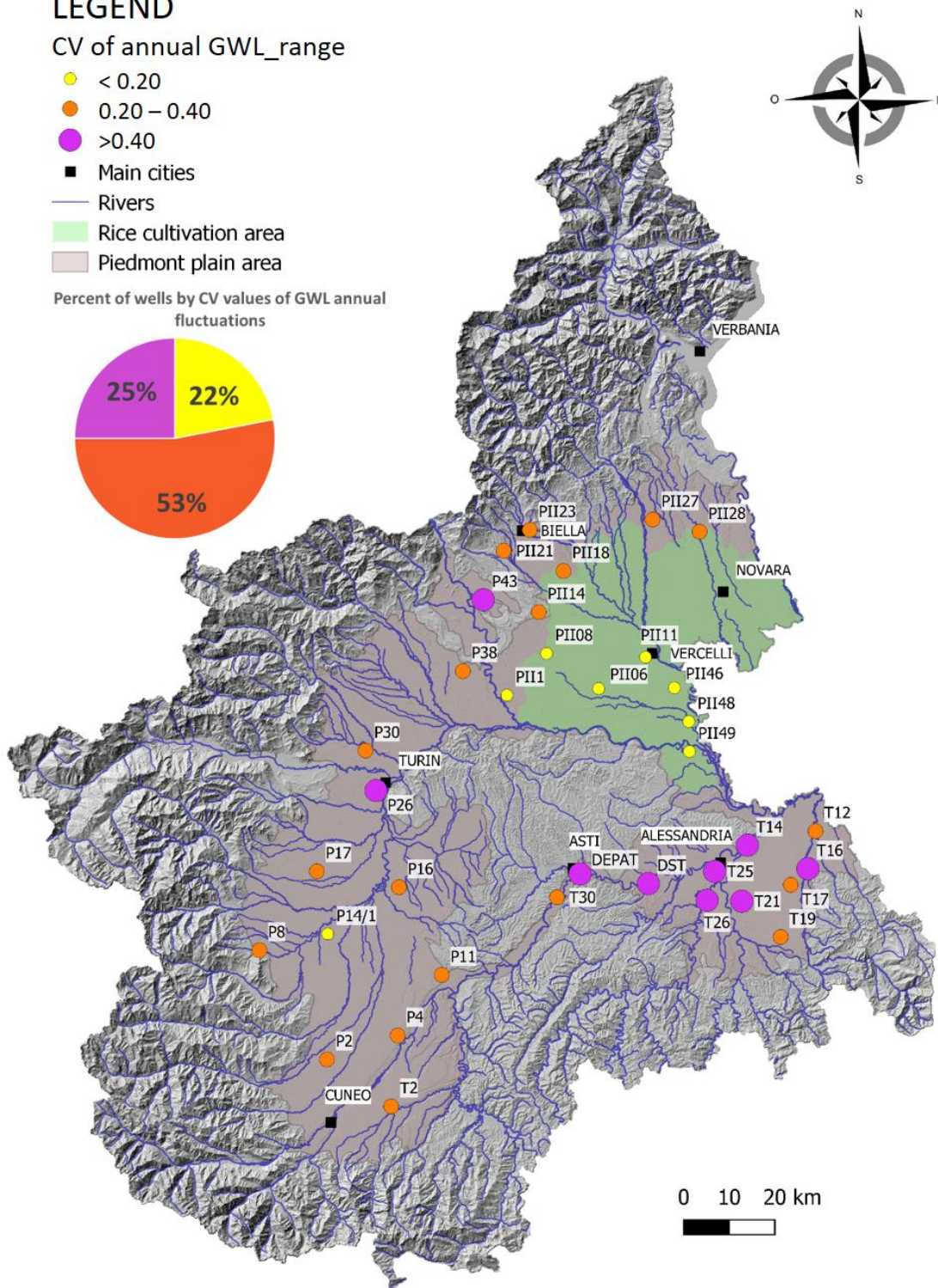
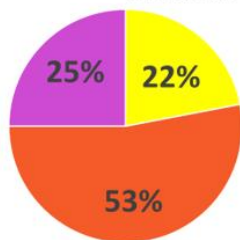
■ Main cities

— Rivers

■ Rice cultivation area

■ Piedmont plain area

Percent of wells by CV values of GWL annual fluctuations

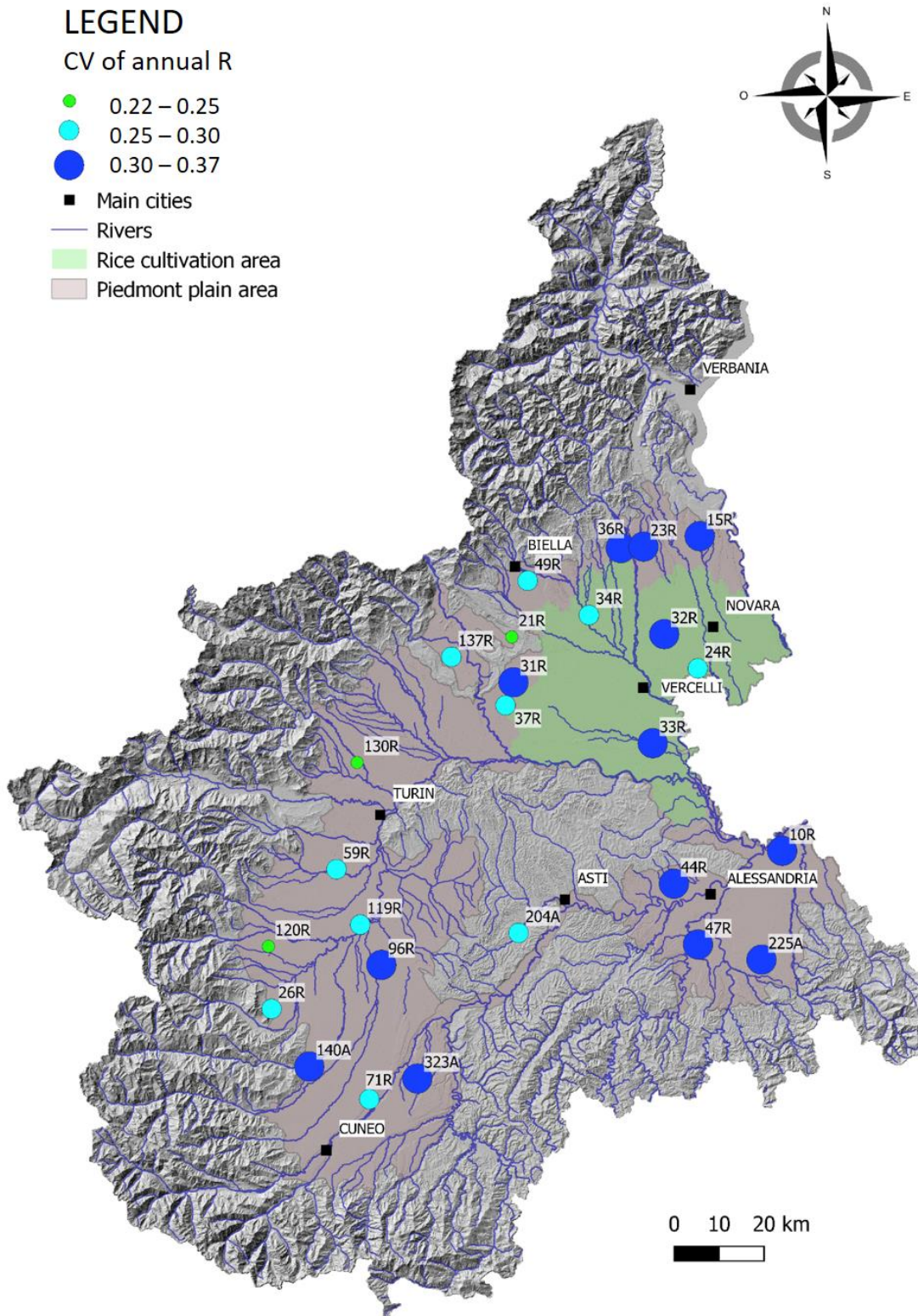


409

410 **Fig. 6.** Spatial distribution of the CV_GWL (CV of annual GWL_range in 2002-2017 period).

411 The interannual variation of R in the period 2002-2017 (CV_R) showed, in some areas, lower
412 values compared to those of GWL amplitudes (Table 2, in supplementary materials). The
413 interannual variation in R in the Piedmont Plain identified a CV_R that varied between 0.22
414 and 0.37. Twelve percent of the annual R time series showed an interannual variation lower
415 than 0.25 ($CV_R < 0.25$), 38% showed CV_R values between 0.25 and 0.30 ($0.25 < CV_R < 0.30$),
416 and 50% showed CV_R values higher than 0.30 ($CV_R > 0.30$) with a maximum value of 0.37.
417 These values are in accordance with the global values observed by Fatichi et al. (2012), ranging
418 between 0.15 and 0.5 in approximately 92% of worldwide rain gauges.

419 The spatial distribution of CV_R showed that the areas with high variation were located in the
420 Alessandria and Cuneo plains and partially in the Novara and Vercelli plains (with $CV_R \geq 0.30$ -
421 0.37). A medium variability of annual R was located along the border with the mountains and
422 in the Turin Plain (with $CV_R \geq 0.22$ -0.30) (Fig. 7)



423

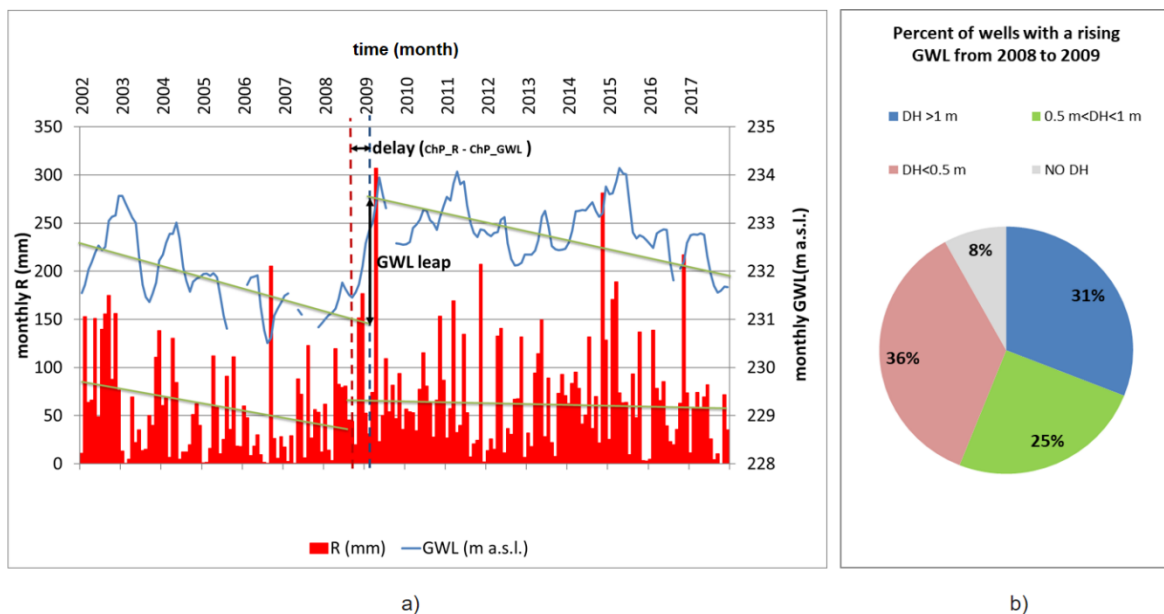
424 **Fig. 7.** Spatial distribution of CV_R (CV of annual R) in 2002-2017 period.

425 **3.2 Change point analysis**

426 The GWL and R data from 2002-2017 were analyzed to identify ChP_GWL and ChP_R in the
 427 time series.

428 Three statistically significant ChP_GWLs occurred in more than 80% of the monitoring wells.
 429 More specifically, the ChP_GWL was observed in 2004-2005 in 81% of the monitoring wells,
 430 in 2008-2009 in 83% of the monitoring wells and in 2015-2016 in 86% of the monitoring wells
 431 (Table 3a, b, c, in supplementary material).

432 The most evident ChP-GWL was in 2008-2009, as also observed in the same study area by
 433 Lasagna et al. (2020b), and corresponds to the transition from a strong lowering followed by
 434 a sudden and considerable increase in the GWL (Fig. 8a). This “leap” was observed in 33 of
 435 the 36 investigated wells. More specifically, the evaluated leap was lower than 0.5 m in 13
 436 monitoring wells, between 0.5 and 1 m in 9 monitoring wells and greater than 1 m in 11
 437 monitoring wells (Fig. 8b).



438

439 **Fig. 8.** a) *change_point GWL time-series (blue line) and R time series (red bar). The dashed*
 440 *vertical lines correspond to the dates respectively of ChP_R (red) and ChP_GWL (blue). The*
 441 *delay between R and GWL correspond to the difference between ChP_R and ChP_GWL*

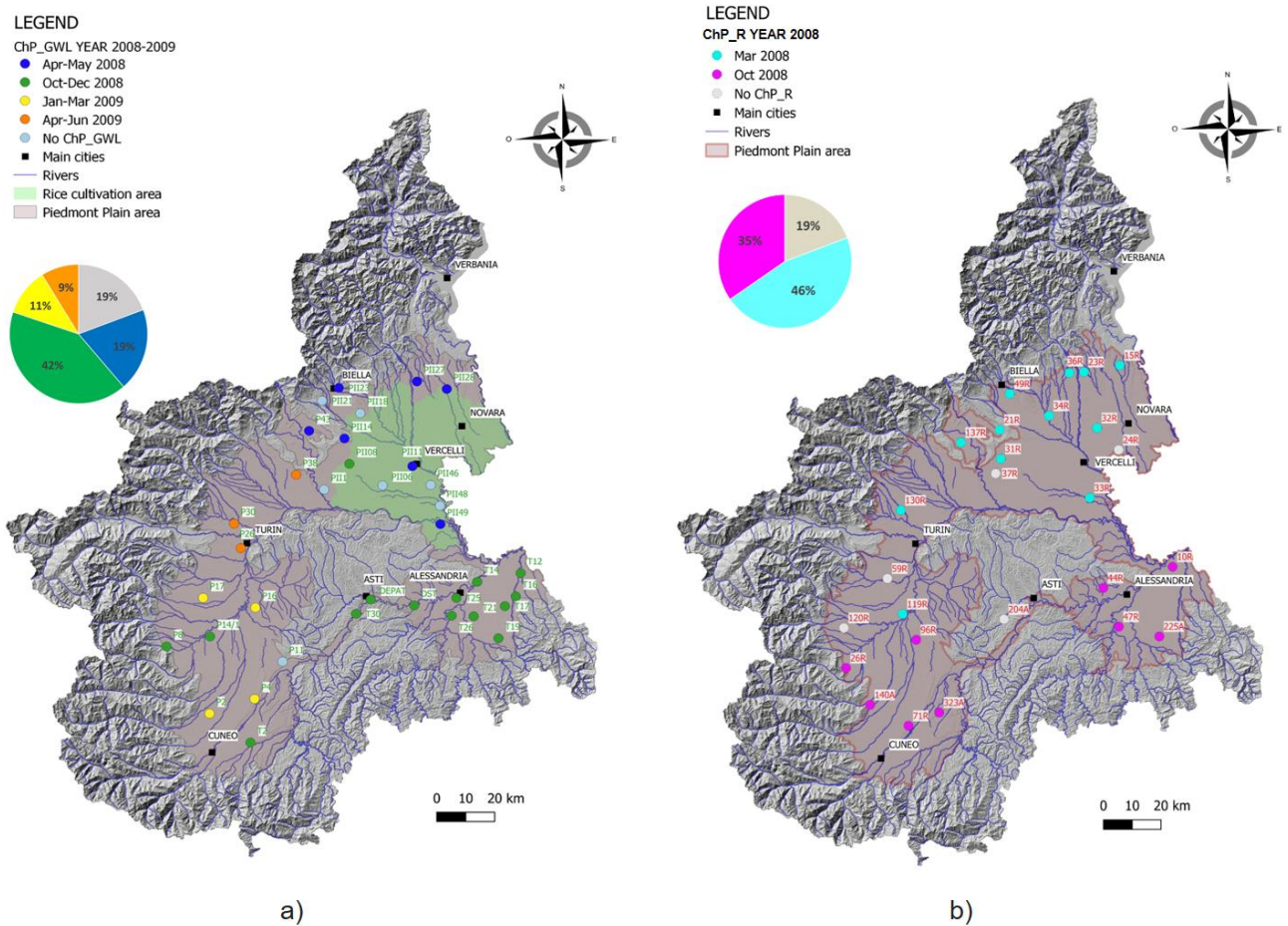
442 *(horizontal black arrow). The vertical black arrow corresponds to the leap of the ChP_GWL*
443 *from 2008 to 2009. b) Percent of wells with a rising GWL from 2008 to 2009, and indication of*
444 *the magnitude of GWL increase (DH) in meter.*
445

446 In the R time series, statistically significant change points (ChP_R) occurred in 19% of the rain
447 gauges for 2004, in 81% of the rain gauges for 2008 and in 23% of the rain gauges for 2015
448 (Table 4, in supplementary materials). The presence of a common change point in most of the
449 GWL and R time series suggests the close dependence of GWL on R.

450 The spatial distribution of ChP_GWL of 2008-2009 allowed us to identify 4 ChP_GWL (Fig. 9a):
451 1) ChP_GWL in April-May 2008; 2) ChP_GWL between October and December 2008; 3)
452 ChP_GWL between January and March 2009; and 4) ChP_GWL in April-June 2009. The first
453 group corresponds to wells located in the northeastern sector of the Piedmont Plain (in the
454 Biella, Novara and Vercelli areas) (20% of the total wells). The second group are wells located
455 mostly in the southeastern sector of the Piedmont Plain (Alessandria Plain) and subordinately
456 in the southwestern sector (Cuneo Plain) (42% of the total wells). The third group consists of
457 wells located in the southwestern sector of the Piedmont Plain (mostly of the Cuneo Plain)
458 (11% of the total wells). Last, the fourth group includes wells located principally in the
459 northern Turin Plain (8% of the total wells). Nineteen percent of the GWL time series showed
460 no ChPs in 2009 and were located mostly in the Vercelli and Biella plains.

461 In the R time series, 57% of the change points detected in 2008 occurred in March, and 43%
462 occurred in October. In particular, change points in March 2008 are referred to as rain gauges
463 located in the central-northern sector of the Piedmont plain (Vercelli and Novara plain, Turin
464 plain); change points in October 2008 are observed in the southern sector of the plain
465 (Alessandria and Cuneo plain) (Fig. 9b).

466 In all cases, ChP_GWL showed a delay from ChP_R. Fifty percent of the delays varied from 0
 467 to 2 months and were detected in the Alessandria Plain and Novara and Vercelli Plains; 22%
 468 of the delays varied from 3 to 6 months and were mostly in the Cuneo Plain and in the Biella
 469 area. Only 3 wells showed a delay higher than 1 year (from 13 to 15 months) and were located
 470 in the northern sector of the Turin Plain.



471

472 **Fig. 9.** Spatial distribution of 2008 a) ChP_GWL and b) ChP_R in the Piedmont Plain and
 473 percent of wells/rain gauges subdivided according to the date on which the ChP occurred.

474 **3.3 Trend analysis results**

475 T on GWL (GWL_T) and R (R_T) were conducted for the entire observation period (2002-2017)
 476 and for the two subperiods obtained by dividing the R and GWL time series at change points
 477 ChP_R and ChP_GWL detected in 2008-2009.

478 GWL_T in the period 2002-2017 highlighted the presence (Fig. 10) of an upwards trend at the
479 $\alpha=0.05$ level of significance in 19% of the total wells (variation between +0.01 m/yr and +0.09
480 m/yr) and a downwards trend at the $\alpha=0.05$ level of significance in 17% of the total wells (-0.01
481 m/yr to -0.14 m/yr). The other 64% of monitoring wells did not show a trend (Table 5a, b, c,
482 d, in supplementary materials). Similar results were found in a previous research conducted
483 on the same study area (Lasagna et al., 2019).

484 The spatial distribution of GWL_T (2002-2017) did not show a trend in the Cuneo and Novara
485 Plains and a variable distribution of positive and negative GWL_T in the other part of the
486 Piedmont Plain. In the Alessandria Plain, the general trend (2002-2017) of the GWL showed
487 negative slopes in almost all cases (even if not statistically significant), with the highest
488 decrease rate (equal to -0.14 m/yr in T17). Only one well showed a positive trend (T25 with
489 an increasing rate of 0.01 m/yr).

490 In the southern part of the Turin Plain, the GWL_T (2002-2017) showed positive trends (from
491 +0.05 to +0.09 m/yr), also in correspondence to the city of Turin. Groundwater level rise in
492 urban areas was observed in many cities in Italy. For example, around the city of Naples
493 (southern Italy) a progressive rising of groundwater levels started since the early 90s, reaching
494 a maximum value of about 14 meters (Allocca and Celico, 2008). The same situation was
495 observed in correspondence to Milan (northern Italy) (Beretta et al., 2004). This phenomenon
496 was generally attributed to a drastic reduction of groundwater withdrawal from public and
497 private wells, formerly used for drinking water, agriculture and industry supplies.

498 R did not show a trend in the period 2002-2017 in all cases (Table 6 in supplementary
499 materials). The same results for R were obtained on the same study area by Lasagna et al.
500 (2019).

501 In the 2002-2008 period, decreasing trends in the GWL series were observed in 89% of the
502 monitoring wells. The other 11% did not show a trend (Fig. 11a). No increase in GWL_T was
503 detected. The magnitude of the negative GWL_T varied from -0.61 m/yr to -0.02 m/yr.

504 The spatial distribution map of GWL_T did not show a trend in the Vercelli and Novara plains.
505 The remaining points in the Piedmont plain showed a small decreasing trend (from -0.04 to $-$
506 0.12 m/yr). Decreasing GWL_T in the Cuneo Plain ranges between -0.05 and -0.20 m/yr (only
507 well P2 showed a strong negative trend of -0.61 m/yr). The highest negative GWL_T was
508 detected in the Alessandria Plain and along the western foot mountains (from -0.10 to -0.42
509 m/yr).








510 Decreasing trends in R in the 2002-2008 period were recorded at 38% of the rain gauges (Fig.
511 11b) and did not show a trend in the other R time series. The magnitude of decreasing R_T
512 varied between -2.4 mm/yr and -10.9 mm/yr.

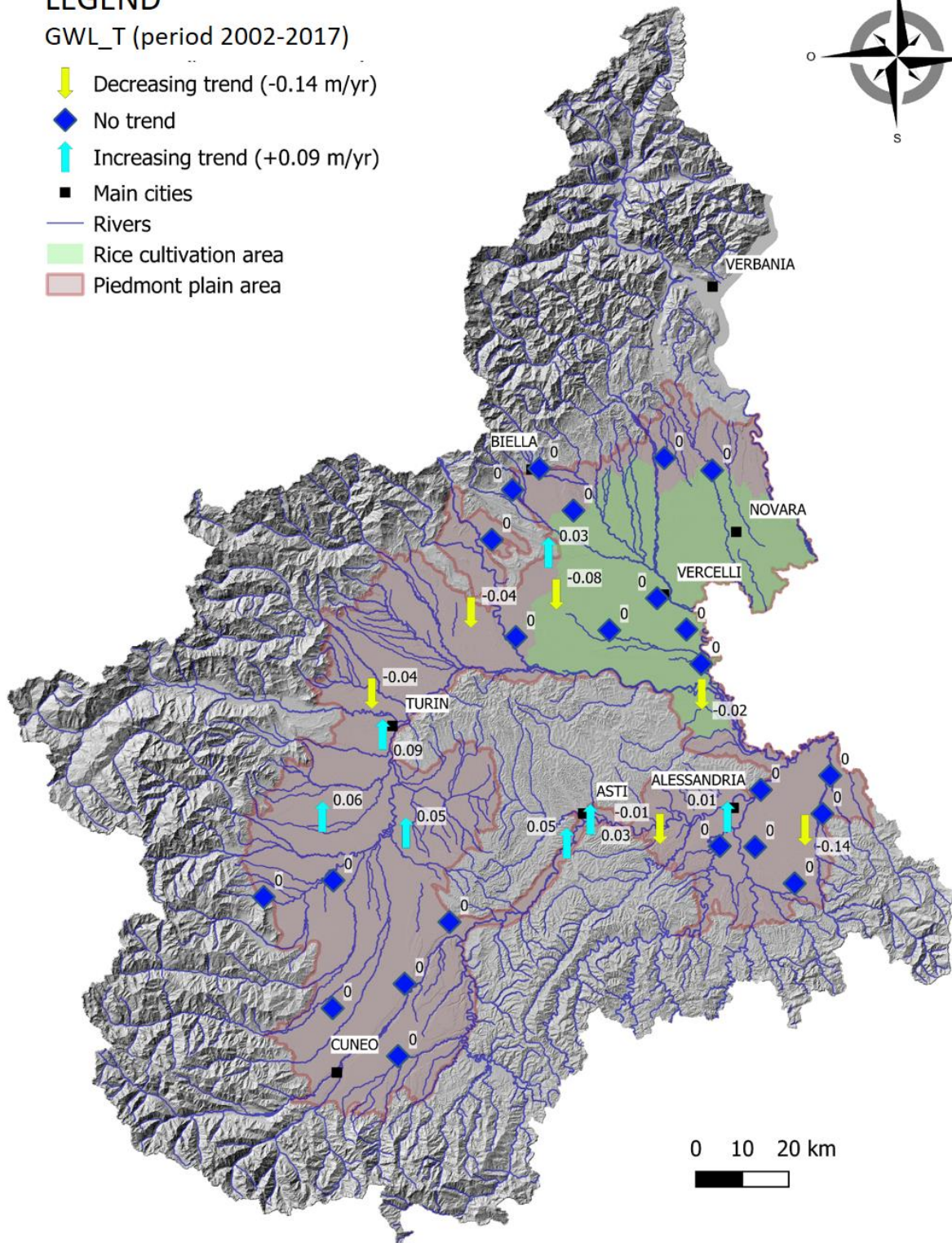
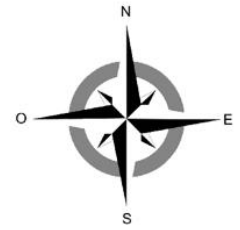
513 In the 2009-2017 period, a decrease in GWL_T was observed in 80% of the monitoring wells,
514 a positive trend in 3% of the monitoring wells and there is not a trend in the other GWL time
515 series (Fig. 12a). The magnitude of decreasing GWL_T varied between -0.02 m/yr and -0.42
516 m/yr. The most pronounced lowering of the GWL is in the Alessandria Plain. In the Vercelli
517 and Novara plains, a decreasing GW_T was present in both the analyzed intervals (2002-2008
518 and 2009-2017), except for the paddy fields area, where there is not a trend in the GWL time
519 series. The same result was obtained by De Luca et al. (2005) for the period 1968-2004.

520 In the 2009-2017 period, decreasing trends in R were recorded at 31% of the rain gauges, and
521 the other 69% did not show a trend (Fig. 12b). The magnitude of decreasing R_T varied
522 between -2.2 mm/yr and -5.6 mm/yr. The negative R_T values were located in the eastern
523 part of the Piedmont Plain.

LEGEND

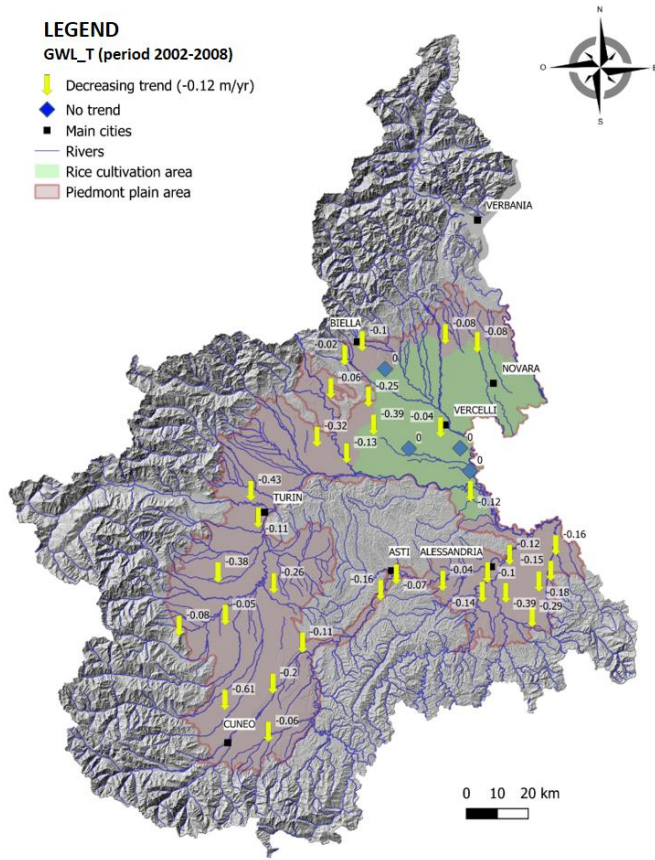
GWL_T (period 2002-2017)

-  Decreasing trend (-0.14 m/yr)
-  No trend
-  Increasing trend (+0.09 m/yr)
-  Main cities
-  Rivers
-  Rice cultivation area
-  Piedmont plain area

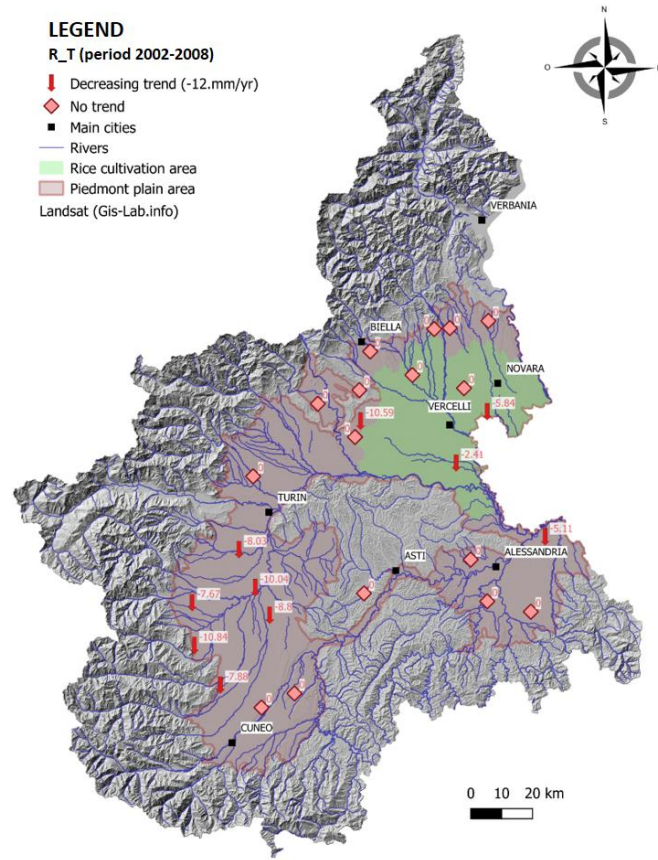


524

525 **Fig. 10.** Spatial distribution of the GWL_T in the 2002-2017 period in the Piedmont Plain. In
526 the 2002-2017 R did not show a trend.



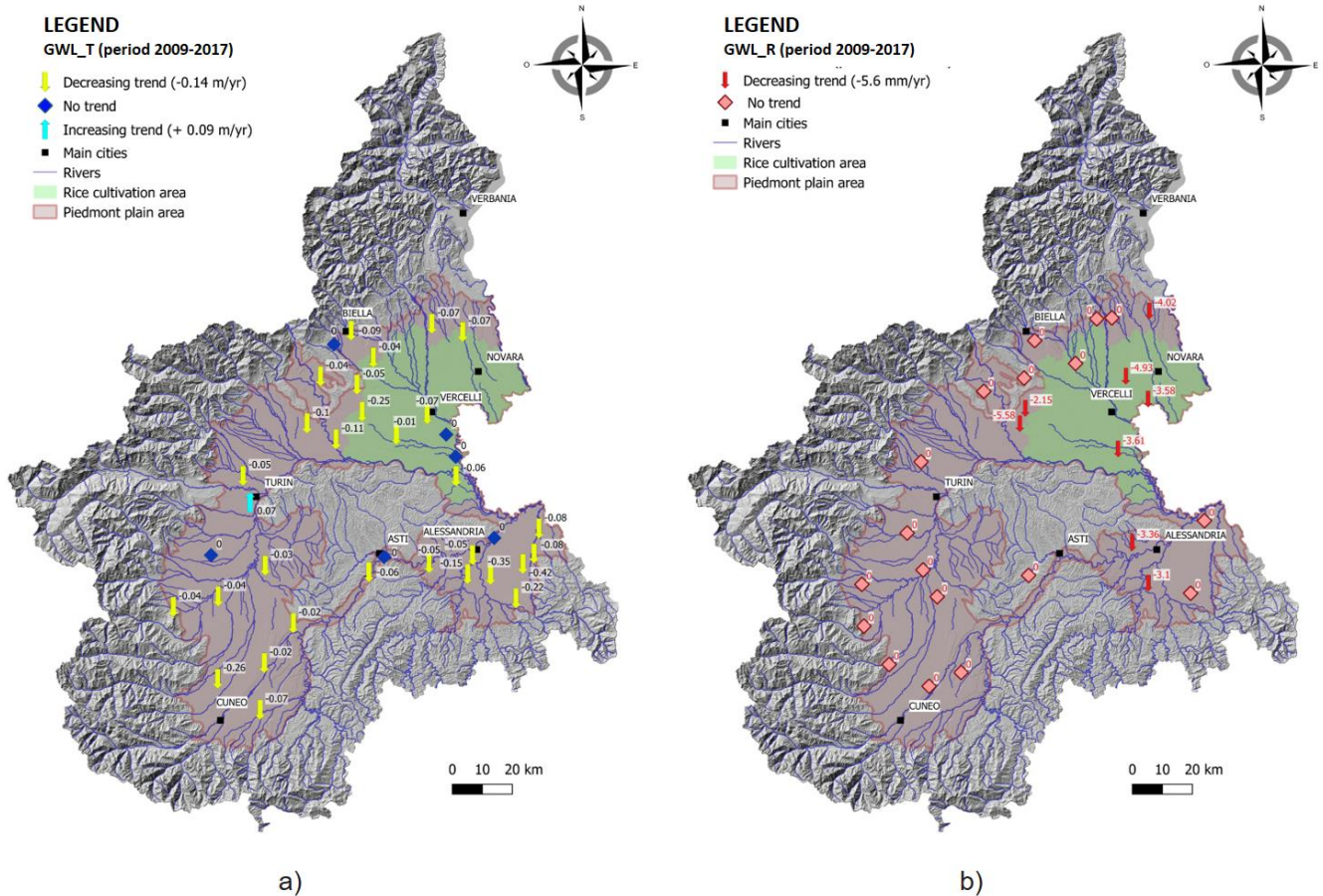
a)



b)

527

528 **Fig. 11.** Spatial distribution of a) GWL_T and b) R_T in Piedmont Plain in the period 2002-2008.



529

530 **Fig. 12.** Spatial distribution of a) GWL_T and b) R_T in Piedmont Plain in the period 2009-2017.

531 **3.4 Percentiles method results**

532 The PCTL method for 2017 highlighted a general situation of GW depletion compared to the
 533 natural fluctuation of GWL. More specifically, only 8% of the monitoring wells had all monthly
 534 GWLs in the range of the natural fluctuation (Fig. 13). These monitoring wells are located in
 535 the western part of the Piedmont plain (south of Turin). Ninety-two percent of wells showed
 536 at least 1 month below the reference threshold (15% of the range of the natural fluctuation)
 537 and were then considered critical: 25% of wells showed from 1 to 4 months, 42% of wells
 538 showed 5-8 months and 25% of wells showed from 9 to 12 months below the reference
 539 threshold. The most critical conditions were found in the southeastern sector of the Piedmont








540 plain (Alessandria Plain). Almost all wells in Alessandria (with the exception of well T14) and
541 Asti plains showed a minimum of 7 months to the full year 2017 below the identified
542 threshold. In this area, the months below the threshold always correspond to the summer
543 and autumn seasons (from May to December).

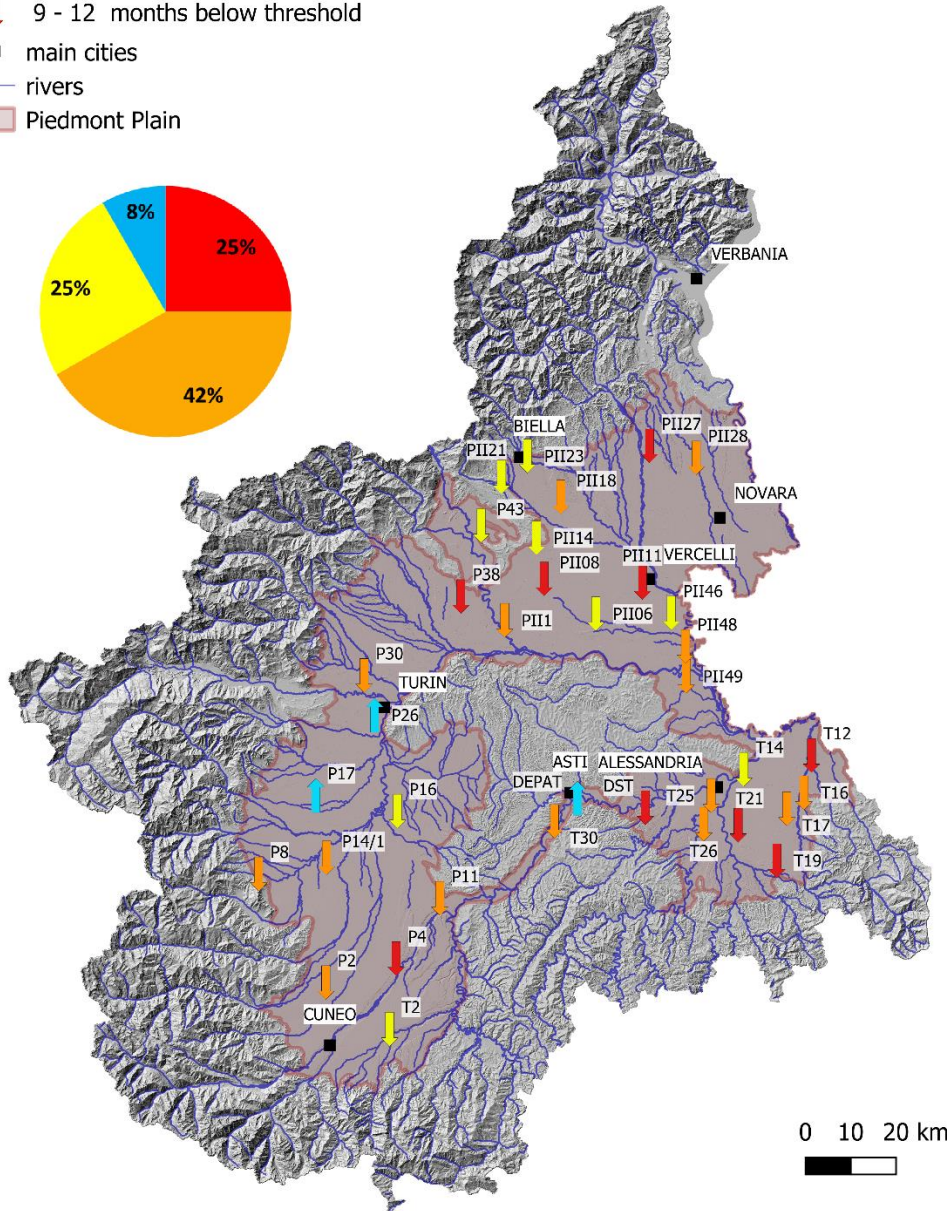
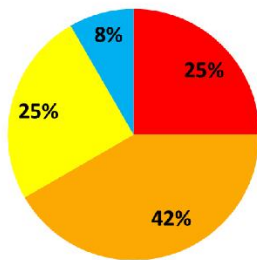
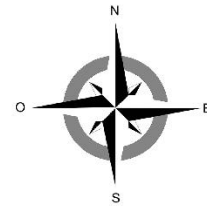
544 In general, in 2017, wells in the Piedmont plain most frequently showed 4 to 6 months below
545 the reference threshold in correspondence with the second part of the year, with more
546 accentuated lowering in the months from April to December (Fig. 14a, b, d). Some wells
547 located in the Vercelli paddy field area are an exception, showing above-threshold values in
548 the summer months (May to September), probably linked to the period of flooding of the
549 paddy fields (Fig. 14c).

550 The wells located in the lowland sector south of Turin mostly showed all months with GWL
551 values above the threshold values (Fig. 14d).

LEGEND

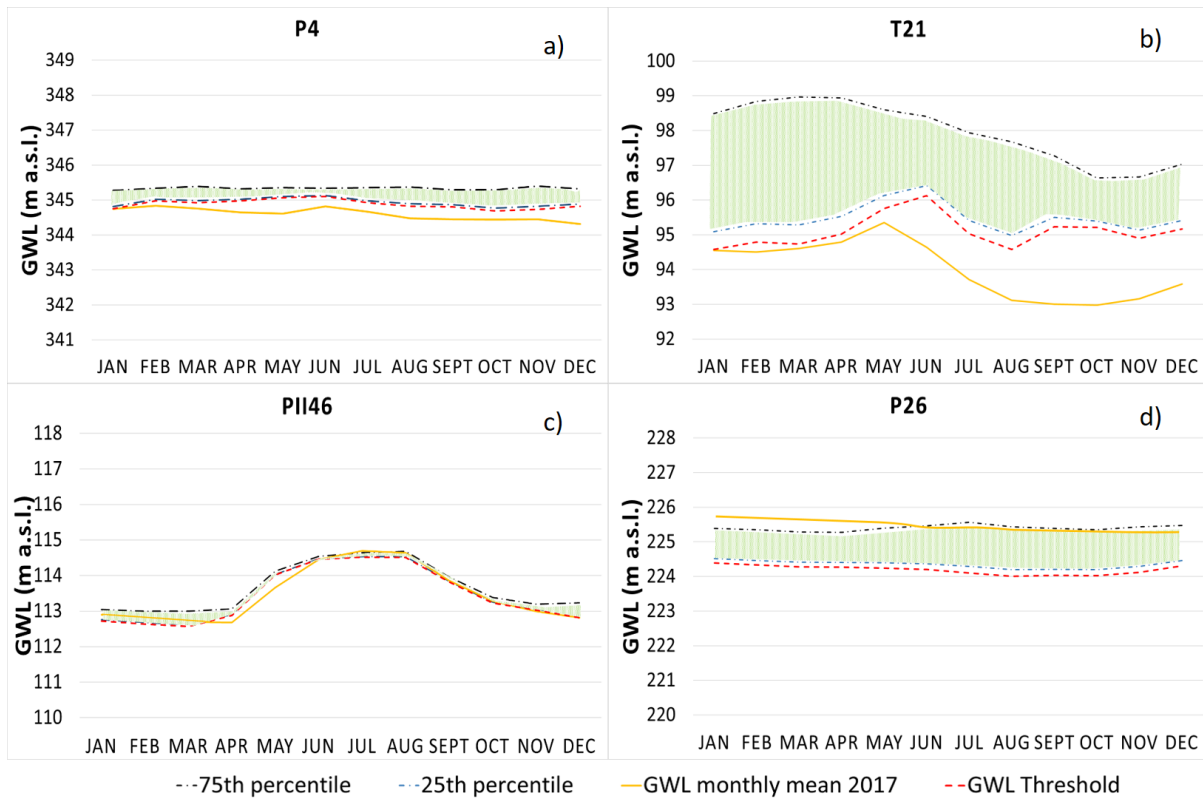
Monthly GWL of year 2017 below percentiles threshold

-  no months below threshold
-  1 - 4 months below threshold
-  5 - 8 months below threshold
-  9 - 12 months below threshold
-  main cities
-  rivers
-  Piedmont Plain



552

553 **Fig. 13.** Spatial distribution of wells with 2017 monthly GWL below the percentile thresholds
 554 (15% of natural fluctuation) and number of months (arrow down). Percent of wells with
 555 number of months with GWL below the percentile threshold.



556

557 **Fig. 14.** a) Examples of monitoring wells with the indication of the 25th and 75th percentiles
 558 (respectively the blue and black dotted lines), the GWL natural fluctuation band (green area),
 559 the “ISPR” threshold computed as 15% of natural fluctuation (red dashed line), and monthly
 560 GWL of 2017 (yellow line): a) Cuneo Plain (P4) with 12 months below the threshold; b)
 561 Alessandria Plain (T21) with 12 months below the threshold c) Vercelli Plain (PII46) with 3
 562 months below the threshold d) Turin Plain (P26) with 12 months above the threshold.

563 **3.5 Non-standardized anomalies**

564 The non-standardized anomalies (or anomalies) allow us to quantify the deviation, positive or
 565 negative, of the GWL from the reference level for each monitoring point.

566 Annual GWL anomalies (GWL_AN) allow us to identify years characterized by GW deficits or
 567 exceeds and to quantify yearly deviations (Fig. 15a, c, e, g). The annual R anomalies (R_AN)
 568 allow the detection of dry and wet years and the quantification of the yearly deviations (Fig.
 569 15b, d, f, h).

570 The analysis of annual GWL_AN for 2017 showed values below the reference levels that varied
 571 between -0.06 and -2.80 m in 92% of wells (Table 7 in supplementary materials). The most

572 critical conditions were located in the southeastern sector of the Piedmont Plain (Alessandria)
573 (Fig. 16a). Only 8% of wells showed an annual GWL_AN above the reference level, with values
574 that ranged between +0.20 m and +0.40 m.

575 The R for 2017 showed, in all cases, negative annual R_AN with values below the rainfall
576 reference levels that vary between -147 and -536 mm (Fig. 16b and Table 8 in supplementary
577 materials). The greatest pluviometric deficits in 2017 were located in the northeastern sector
578 of the Piedmont Plain (Novara and Vercelli).

579 In 2017, the spatial distribution of GWL_AN generally showed different values in the different
580 sectors of the Piedmont Plain.

581 In the Novara and Vercelli paddy field areas, the yearly GWL_AN was close to the reference
582 level (Fig. 15a), and in 2017, all the monitoring wells, except for PII08, had anomalies less than
583 0.6 m (Fig. 16a).

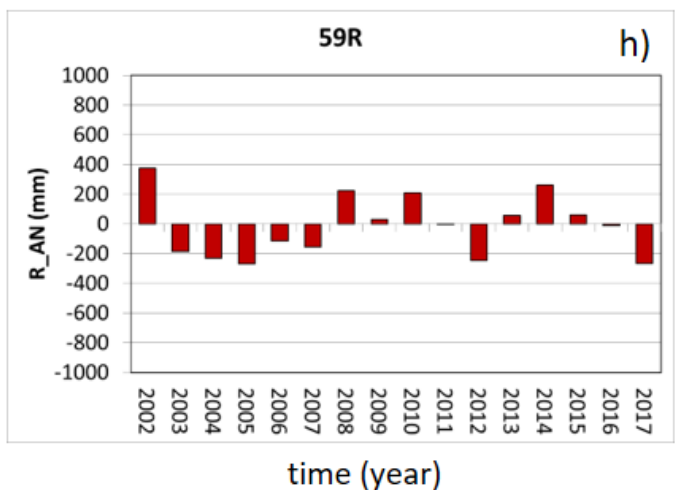
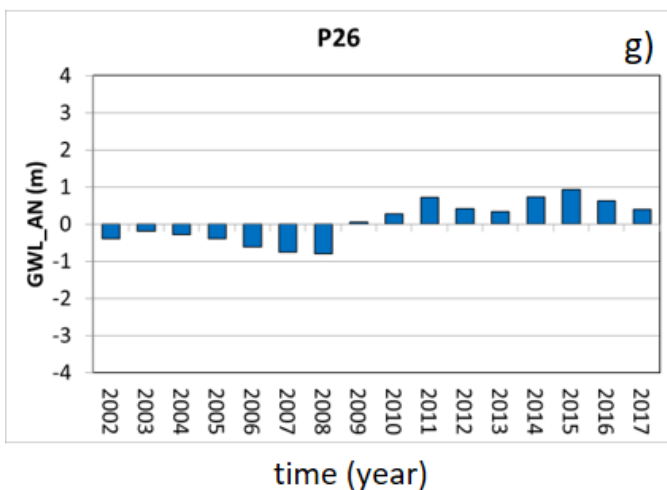
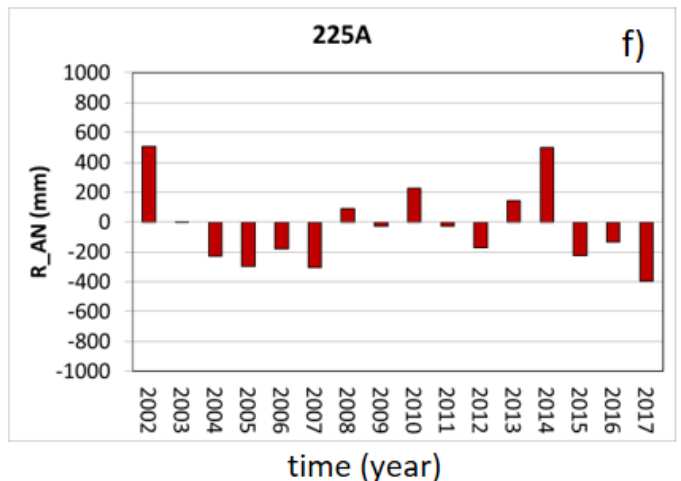
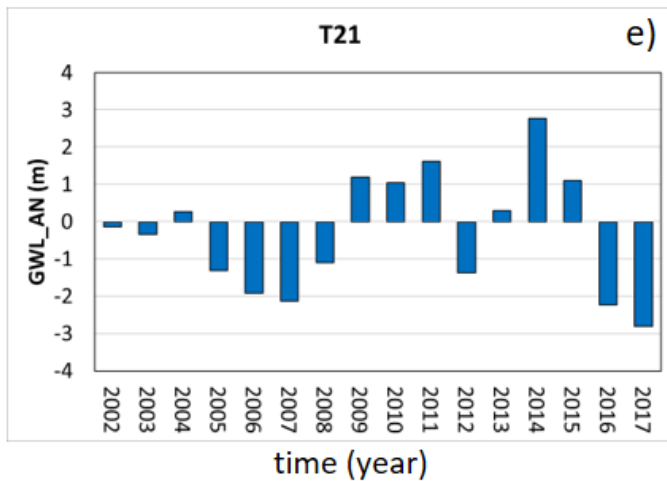
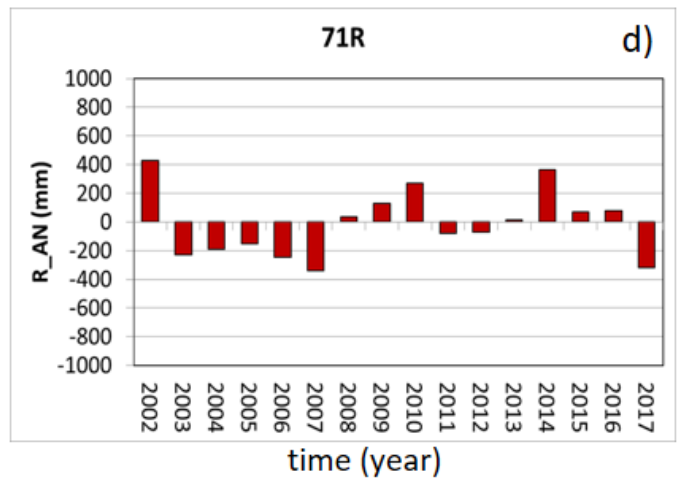
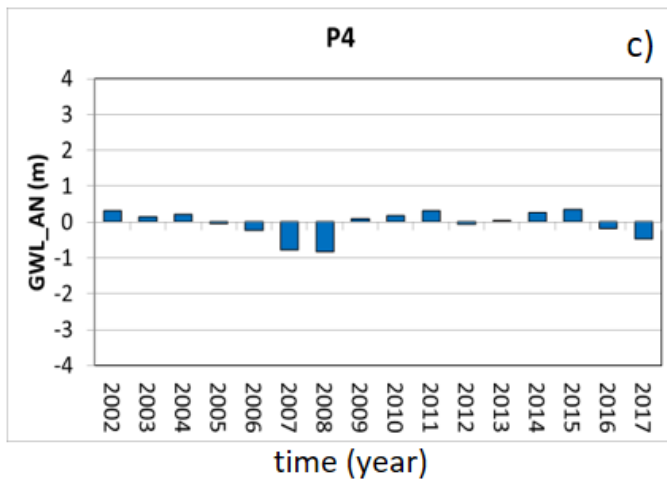
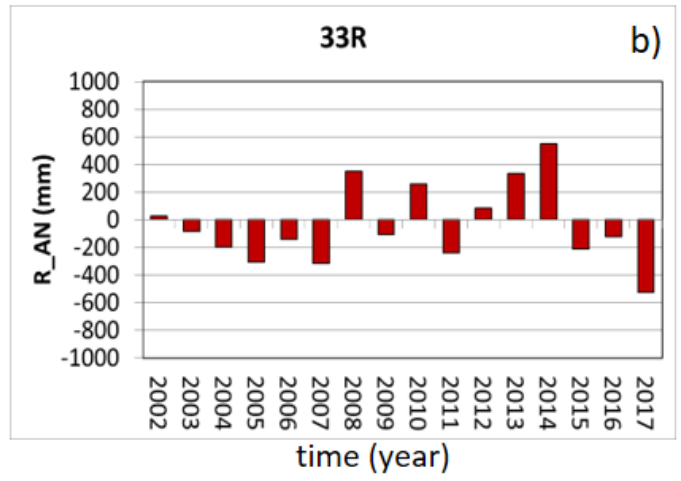
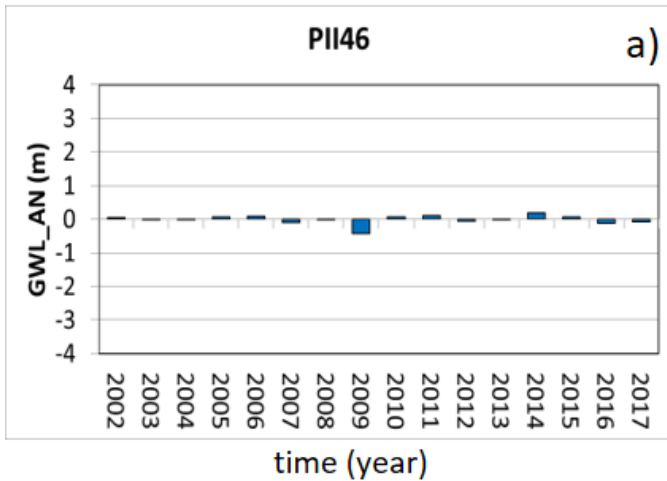
584 In the Cuneo Plain, the yearly GWL_AN was nearly the reference level but, in general, was
585 more pronounced than in the Vercelli Plain (Fig. 15c), and in 2017, all the monitoring wells
586 showed a negative GWL_AN of less than 0.8 m (Fig. 16a).

587 On the Alessandria Plain, the yearly GWL_AN showed the highest negative values, and in
588 2017, several monitoring wells showed negative GWL_AN values of more than 1.4 m up to
589 2.8 m (Fig. 16e). The wells located in the Tanaro valley showed a 2017 GWL_AN of a few tens
590 of centimetres (0.10-0.30 m) (Fig. 16a).

591 Positive and negative GWL_AN were detected in some wells in the southern part of the Turin
592 Plain (Fig. 15g and Fig. 16a) with annual values lower than 0.4 m in 2017.

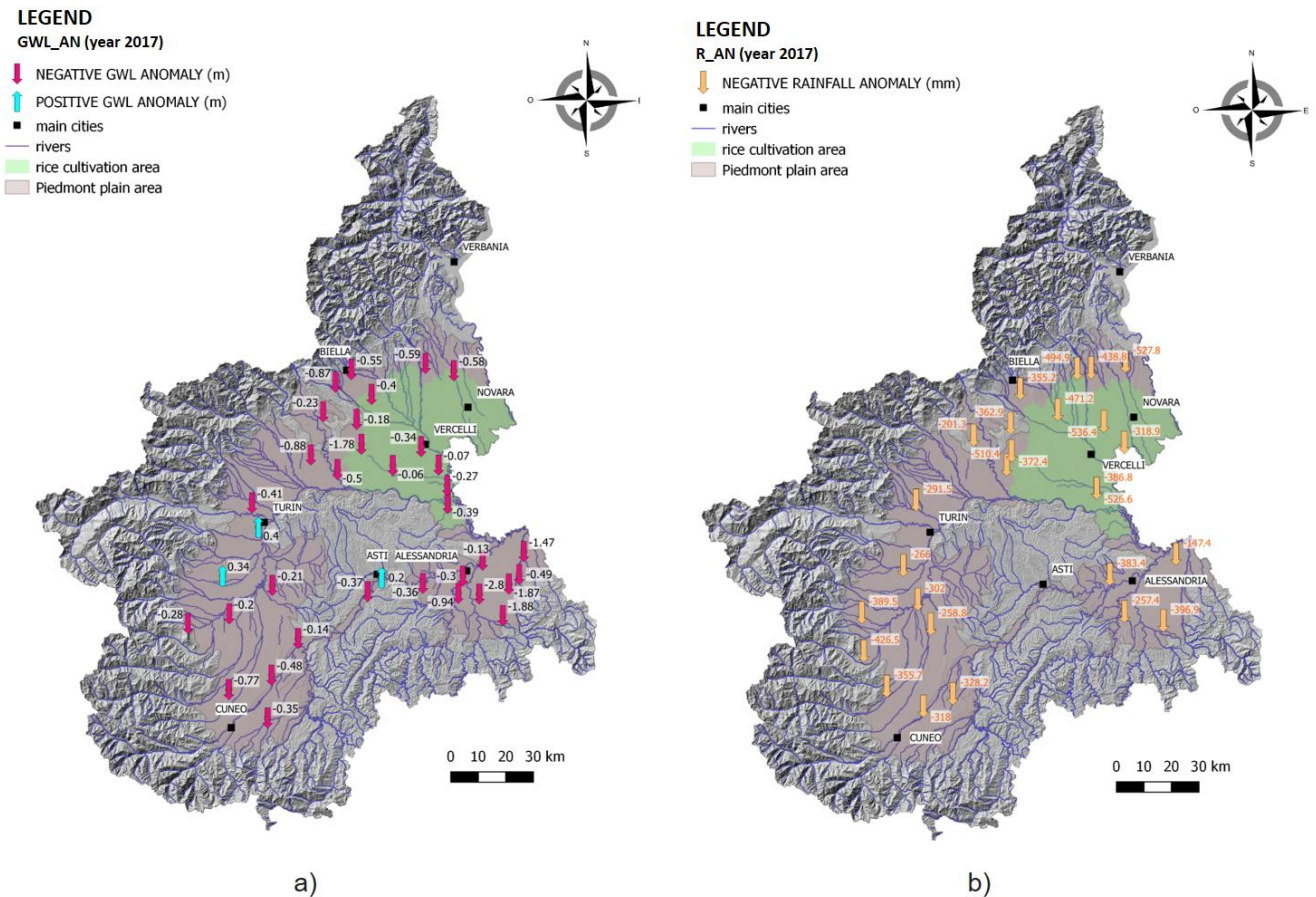
593 The comparison of annual R_AN with GWL_AN shows that large R_AN values do not always
594 correspond to large GWL_AN values. Generally, R_AN had the same sign as GWL_AN (Fig. 15
595 b, d, f, h). Sometimes, it was possible to observe a lag of 1 year.

596 A positive R_AN corresponded to the wet period and was observed in 2002, 2008-2011 and
597 2013-2014. Negative R_AN, corresponding to the dry period, was observed in 2003-2008 and
598 in 2017. The years 2015 and 2016 showed a positive R_AN in the Turin and Cuneo Plains
599 (western Piedmont Plain) and a negative R_AN in the Vercelli and Alessandria Plains (eastern
600 Piedmont Plain).



602 **Fig. 15.** Annual GWL_AN (blue bar) and annual R_AN (red bar) of monitoring wells and
 603 correspondent rain gauges, respectively: a) and b) in the Novara-Vercelli Plain; c) and d) in the
 604 Cuneo Plain; e) and f) in the Alessandria Plain; g) and h) in the Turin Plain.

605



606
 607 **Fig. 16.** Spatial distribution for the year 2017 of a) GWL_AN. Negative GWL_AN (red arrow
 608 down) and positive GWL_AN (blue arrow up); b) R_AN. R showed, in all cases, a negative
 609 anomaly (yellow arrow).

610

611 4. DISCUSSION

612 The application of different methods (such as T, ChPA, PCTL, AN and the analysis of annual
 613 fluctuations and their variations over time) to the GWL series of the Piedmont Plain allowed
 614 us to assess the GWL evolution over time.

615 Variations in GWL depend on many factors related to the hydrogeological context, climate
616 and anthropogenic pressures and their variability over time. Moreover, the application of
617 these methods to the R time series also allowed the comparison between R and GWL results,
618 providing further information on the hydrodynamic behaviour of groundwater and on its link
619 with R variability.

620 Furthermore, the spatialisation of the GWL elaborations allowed us to identify the most
621 critical areas and the potential factors (anthropic, geological and hydrogeological)
622 conditioning the hydrodynamic GWL behaviours.

623 Finally, this multicriteria approach, considering the same time interval, allowed us to highlight
624 the advantages and limits of the applied methods.

625

626 **4.1 The evolution of the GWL**

627 The T conducted in the period 2002-2017 indicate that all rain gauges and approximately half
628 of the monitoring wells did not show any trend. Nineteen percent of the total wells showed a
629 positive trend, and only 17% of the total wells showed a negative trend. Since the results of T
630 depend on the time interval considered, especially in cases where the slopes are not
631 accentuated and in the case in which the interval is not so long, it was useful to search for
632 change points to define the beginning or the end of the analysis intervals.

633 The presence of the change point in 2008 allowed us to divide the time series into two parts,
634 and T was applied to the two subperiods showing a general decreasing trend in more than
635 80% of wells and in less than 35% of rain gauges. Generally, the negative GWL_T detected in

636 2009-2017 showed fewer negative slopes than those detected in 2002-2008. Moreover,
637 aquifer responses also seem to be different in similar climatic areas.

638 The trends obtained for the second subperiod (2009-2017) were comparable with the results
639 obtained by applying the percentile method and the non-standardized anomaly method.

640 The PCTL highlighted a general situation of GW depletion in only 11% of wells showing a
641 piezometric level above the threshold and in the range of the GWL natural fluctuation. The
642 analysis of GWL_AN for 2017 confirmed the results of percentiles, showing annual values
643 below the reference level that vary between 0.2 and 2.8 m in 92% of wells (Table 7 in
644 supplementary materials). Moreover, percentile analysis for 2017 showed that the greatest
645 GW deficits generally occurred in the second part of the year.

646 The R for 2017 showed, at all rain gauges, negative anomalies that varied between -147.26
647 mm in the Alessandria Plain and -585.21 mm in the northern area of the Piedmont Plain
648 (Novara and Vercelli areas). This deficit in the R can be the cause of the GW depletion in 2017.

649

650 **4.2 Comparisons and relationships between R and GWL fluctuations**

651 The analysis of the maximum amplitude of annual GWL fluctuation (GWL_range) showed that
652 this value varies over time and that most of the analyzed wells had an average GWL_range
653 lower than 2 m (80% of the wells). During the analyzed period, the maxima of GWL_range
654 were generally observed in the years 2002-2003 for 47% of the monitoring wells and
655 secondarily in 2009 (8%) and 2013-2014 (14%); minimum values of GWL_range were, instead,
656 more distributed over the years. However, a high presence of the minimum GWL_range in
657 2007 and 2013 can be observed (Table 1 in supplementary materials). To explain the periods

658 of maxima and minima annual amplitude of GWL fluctuations, a comparison with average
659 annual R was performed.

660 The high fluctuations in the highlighted periods can be ascribed to particularly high R (up to
661 1400 mm/yr) or low R (less than 800 mm/yr) with respect to the average annual R in the
662 Piedmont Plain (911 mm/yr, Fig. 2). Periods of high R are effectively identified in 2002, 2008-
663 2010 and 2014, whereas low R are measured in 2003-2007 and 2017. In contrast, the
664 minimum amplitude of annual GWL fluctuations seems not linked to periods of particularly
665 elevated or low R.

666 The CV_GWL allowed us to evaluate the interannual variation degree of the GWL_range in
667 each monitoring well. Then, the spatialisation of the CV_GWL allowed us to identify areas
668 with the highest interannual variation ($CV_GWL > 0.40$ in the Alessandria Plain), areas with the
669 lowest interannual variation ($CV_GWL < 0.20$ in the Vercelli and Novara plains) and areas with
670 intermediate CV_GWL values ($0.20 < CV_GWL < 0.40$). The interannual variation in R showed
671 medium-high CV_R values (from 0.22 to 0.37), with the highest variations in the Alessandria,
672 Cuneo, Novara and Vercelli plains.

673 By comparing CV_GWL and CV_R, it was possible to distinguish areas with comparable
674 interannual variability. The highest values of CV_GWL and CV_R were detected in the
675 Alessandria Plain, suggesting a rather close link between R and GWL variation; however, the
676 variation in the annual cumulative R was lower than the variation in the annual excursion of
677 the water table ($CV_GWL > 0.40$ and $CV_R > 0.30$).

678 In contrast, in the Novara and Vercelli plains, it was observed that the annual GWL_ranges
679 varied little over time ($CV_GWL < 0.20$) and, in any case, were less than the variability in R
680 ($CV_R > 0.30$). The low CV_GWL could be explained by systematic paddy field flooding (Lasagna

681 et al., 2020b), which influences and controls the variations in the water table in the spring-
682 summer period. The water used for the permanent flooding of the rice fields is derived from
683 rivers in the northern part of the area and through a network of channels managed by local
684 irrigation authorities.

685 The analyses of change points in GWL and R highlighted a common change point in 2008-2009
686 for most analyzed series. This testifies that the water table oscillation is ruled more or less
687 evidence by R, which is expected. Most specifically, the highlighted rise in the GWL in 2008-
688 2009 can be explained by a considerable increase in precipitation. Observing the annual R in
689 the Piedmont plain, it is possible to point out that 2007 was a particularly dry year (with
690 average R values below 650 mm), while 2008 was a rainy year (with average R values above
691 1100 mm). In addition, according to what was reported by ARPA (Arpa, 2016), 2008 was, on
692 a regional scale, the second year with the largest anomaly of positive snowfall since 1950.
693 Consequently, it cannot be excluded that the melting of these snows contributed to the rapid
694 rise recorded in 2009. However, this does not mean that the variations in the GWL are due
695 exclusively to precipitation. In all cases, Chp_GWL shows a delay time compared to the dates
696 of ChP_R. Minor delays (0-3 months in the Alessandria and Novara and Vercelli Plains) could
697 indicate a speed recharge of the aquifer by R, favoured by depths of GWL and high
698 permeability of the unsaturated soil. Higher delays (over 3-6 months) could indicate a higher
699 influence of further factors in addition to rain, such as permeability of the unsaturated soil,
700 depth of the water table, snow melt, irrigation, and anthropic water depletion. For example,
701 well P38 has the greatest depth of the water Table (47 m) and has a delay of more than 12
702 months.

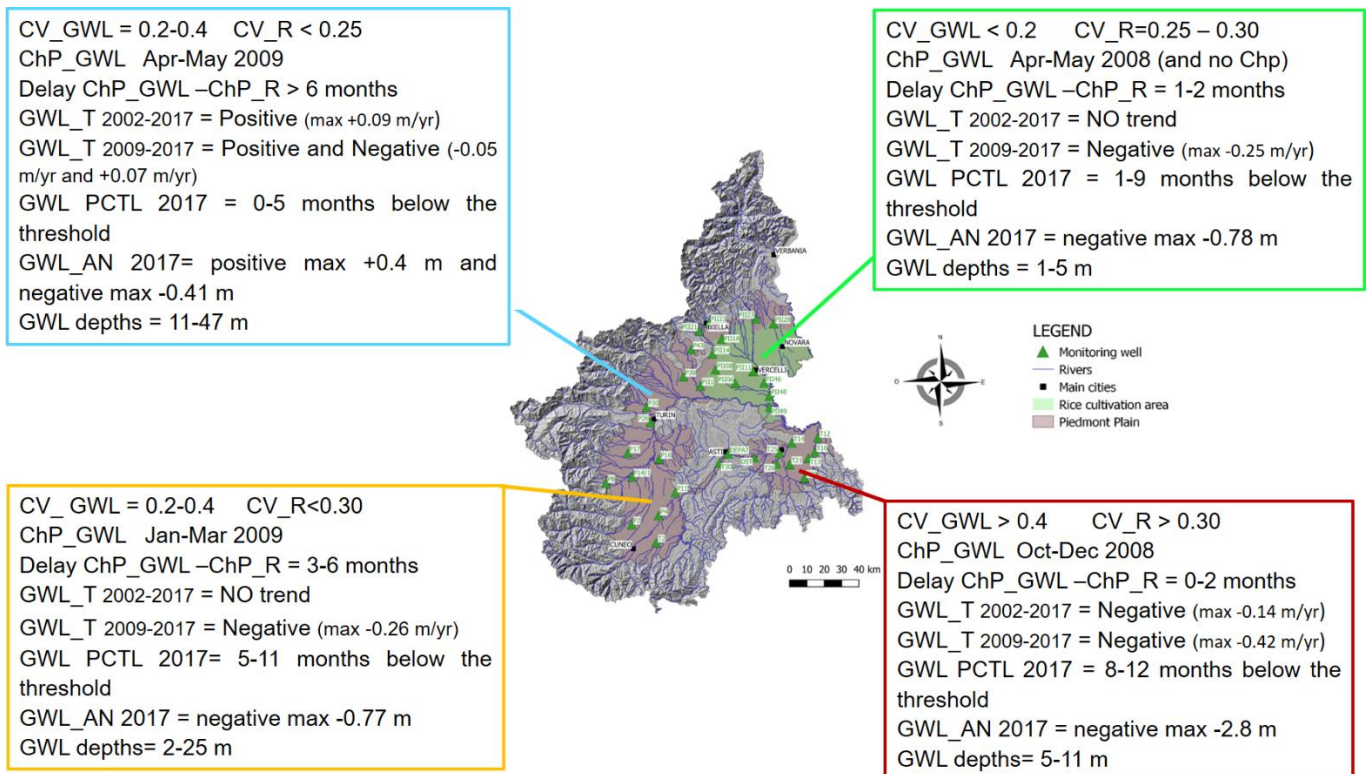
703

704 **4.3 Quantitative status of GW resources in the Piedmont Plain**

705 The analysis of the GWL over time permitted us to define the quantitative status of the GW
706 resources for 2017, identifying 4 different plain areas with similar behaviours (Fig. 18):

- 707 a) Southeastern sector (Alessandria plain),
- 708 b) Northeastern sector (Vercelli-Novara plain with rice fields),
- 709 c) Northwestern sector (Turin plain),
- 710 d) Southwestern sector (Cuneo Plain).

711 It should be noted that 2017 in the Piedmont Region was the 3rd warmest year in the last 60
712 years, with a thermal anomaly of approximately +1.5 °C compared to the climatology of the
713 period 1971-2000 and the 4th driest year of the last 60 years (Arpa, 2018). However, aquifer
714 responses also seem to be different in similar climatic areas.



715

716 **Fig. 17.** *Summary of the main results of the different statistical elaborations and*
717 *identification of 4 sectors, of the Piedmont plain, identified by similar CV, trends, delays and,*
718 *GWL_AN.*

719 Southeastern sector (the Alessandria plain)

720 The Alessandria plain is located on the border with the Apennine chain and is characterized
721 by a local climate that is different from the other parts of the Piedmont Plain. More
722 specifically, it is characterized by the lowest average annual R (of the Piedmont Plain) and the
723 highest summer temperatures (which probably also intensify water withdrawals in the area
724 as well as affect evapotranspiration). The particular location and geometry of the aquifer are
725 characterized by a small areal size, as it is surrounded to the northwest and south by the BTP
726 sedimentary rocks.

727 In 2017, all the methods applied to the GWL identified a critical situation in this plain. R
728 variations and other factors, such as the increase in withdrawals from the aquifer principally
729 due to the drought that characterized this area (Regione Piemonte, 2020), are likely to
730 contribute to the pronounced decline in GWL.

731 All GWL_T analyses showed the maximum negative slope (max=-0.42 m/yr for GWL_T₂₀₀₈₋₂₀₁₇)
732 in the Alessandria Plain, and percentile analysis and GWL_AN (max= -2.80 m) identified the
733 most critical conditions in this area (for 2017). The analysis of the interannual variation in
734 GWL_range and annual R amounts showed the highest values in the Alessandria Plain
735 (CV_GWL>0.40 and CV_R>0.30), suggesting a rather close link between R and GWL variation.

736 The GWL depths in this area are between 5 and 11 m below the ground surface, and these
737 data can in part justify the low time response (0–2 months) of the GWL to R.

738 Northeastern sector (Vercelli-Novara plain)

739 The northeastern sector of the Piedmont Plain is characterized by an average depth of the
740 water table lower than 5 m below the ground surface and a generally high hydraulic
741 conductivity of soils (De Luca et al., 2020). The aquifer is bounded to the north by the
742 mountain chains of the Alps and to the south by the Monferrato hills, at the base of which
743 flows the River Po. The Vercelli and Novara areas were largely characterized by the presence
744 of paddy fields that were subject to repeated flooding phases during the period from April to
745 August. During flooding, the water table is artificially fed, thus reducing/masking any
746 criticalities arising from a scarce natural recharge.

747 The Novara and Vercelli plains showed the highest annual R compared to other areas of the
748 Piedmont Plain. The GWL_T analysis in this area did not show a trend for the period
749 (GWL_T₂₀₀₂₋₂₀₁₇) but a negative trend in the second subperiod (GWL_T₂₀₀₈₋₂₀₁₇), with most
750 slopes below 0.1 m/yr. The time response of GWL to R varies from 1 to 2 months and seems
751 to indicate that the effects of R become evident quickly. Despite the shallow water table and
752 the high hydraulic conductivity of the soils, the time response is greater than those evaluated
753 in the Alessandria area, where the water table is mostly deeper and the hydraulic conductivity
754 is similar. Furthermore, the interannual variability in GWL_ ranges in this area is the lowest in
755 the Piedmont Plain (CV_GWL <0.2).

756 These effects could be explained by the artificial water supply that influenced and conditioned
757 the course of the GWL during the summer period and helped to reduce the annual amplitude
758 of GWL fluctuations, which, under natural conditions, would probably have been much higher
759 (Lasagna et al., 2020b).

760 North-Western sector (Turin Plain)

761 The Turin Plain, between the Alpine edge to the west and Turin Hill to the east, is the
762 connecting element between the Cuneo Plain and the rest of the Po Valley. It is bordered to
763 the west by the morainic apparatus of Rivoli-Avigliana and to the east by the hills of Turin.
764 The subsoil has a prevalent permeability for medium grade porosity, with a frequent lower
765 degree of hydraulic conductivity, especially in the oldest and altered terms ($10^{-7} < k < 10^{-3}$ m/s)
766 (De Luca et al., 2020). The average depth of the water table is higher than 10 m, up to 40 m
767 below the ground surface. The analyses conducted on the wells present in this area showed
768 different results compared to those found in the other areas. In the southern sector,
769 increasing trends have been identified both for the long period (2002-2017) and for the last
770 subperiod (2009-2017); moreover, the GWL of 2017 was higher than the reference threshold
771 calculated with the method of percentiles, and the annual GWL_AN anomalies also showed
772 positive values (up to 0.4 m), despite the rain presenting negative annual R_ANs. The average
773 GWL_range was generally less than 2 m, and CV_GWL had intermediate values ($0.2 < CV < 0.4$).
774 This area is where the highest delays in the response of the GWL to R occur (over 6 months).
775 These data could be related to deep GWL, with soils characterized by medium-low hydraulic
776 conductivity. However, other factors could also likely explain this different behaviour.

777 The particular position of the lowland area with respect to the Alpine arc suggests that,
778 perhaps, a nonnegligible water contribution could be derived from snow melt. This further
779 contribution could partly explain the positive trends observed in the area and the moderate
780 CV_GWL.

781 South-Western sector (Cuneo Plain)

782 In the Cuneo Plain, the average depth of the water table is highly variable (from a few metres
783 up to 24 m). In wells with a shallower water table, the amplitude of the GWL_range oscillation

784 seems to be lower (<1 m) than in wells with a deeper water table. The interannual variation
785 in the maximum amplitude of GWL fluctuations is intermediate ($0.2 < CV_{GWL} < 0.4$) and
786 comparable to CV_R ($CV_R = 0.3$). However, the delays between ChP_R and ChP_{GWL} varied
787 from 3 to 6 months. This delay in the GWL response to R may be related to the depth of the
788 water table.

789 The GWL_T analysis in this area did not show a trend for the long-term period observed (2002-
790 2017) but a negative trend in the last subperiod (2009-2017) with slopes of -0.26 m/yr. The
791 PCTL analysis applied for 2017 showed at least 5 months below the reference threshold in all
792 wells, and negative GWL_{AN} was detected (max -0.77 m). The slightly negative trends
793 recorded in the last period and the more negative anomalies calculated for 2017 can also be
794 explained in this case, as for the Turin Plain, by a water contribution that could derive from
795 snow melt.

796 **4.4 Advantages and disadvantages of applied methods for GWL analyses**

797 It is important to emphasize that all the analyzed methods, to have good and significant
798 applicability, require a rather high number of years of measurement (on average of at least 5
799 years, to many decades (ISPRA, 2017)). Additionally, continuity over time of measurements is
800 necessary, and the lack of continuity of the data as well as the high presence of missing data
801 can distort the results. Furthermore, to make comparisons between the results of the
802 elaborations, it is important to consider the same time interval.

803 The analysis of change points is useful for determining the moments when a change in trends
804 is observed and allows the subdivision of the time series into smaller intervals. In addition,
805 the change points search can be useful to identify and compare moments common to

806 different time series (i.e., between R and GWL) and to evaluate the possible delay in
807 responses. Last, the change points are sensitive to the length and time period analyzed.

808 The evaluation of the trends is simple and can be usefully interpreted in association with GW
809 status data. T gives an idea of the evolution of the GWL over time. However, the evaluation
810 of a statistically significant T, above all when the T line does not present a high slope and in
811 the presence of not a very long temporal series, is strongly dependent on the analyzed period
812 (Mariani, 2018); thus, the choice of the reference period appears to be a key element for the
813 analysis of trends. Moreover, it is advisable to evaluate the presence of change points in the
814 GWL series and to evaluate the trends in different time intervals. Common change points
815 detected in different time series can be considered starting (or finishing) points for T. T for
816 the assessment of climate change impacts on groundwater recharge, groundwater level and
817 resources, requires a long time interval (e.g. more than 30 years), but the observation data,
818 e.g., groundwater levels are generally not available. Moreover, short-term T series can be
819 used to assess the effects of climate variability and provide useful information on aquifer
820 recharge patterns.

821 The percentile method proposed by ISPRA establishes an alert threshold below which the
822 GWL is considered critical. Furthermore, the percentile method shows intuitive diagrams.
823 However, it does not convey the extent of GW depletion. The warning threshold is
824 determined on the basis of the amplitude of the "natural fluctuation". In the cases where the
825 amplitude of the 'natural fluctuation' band is low, the threshold will be close to the 25th
826 percentile, and a GWL below the defined threshold does not always correspond to a real
827 criticality.

828 The assessment of the magnitude of the annual GWL_range fluctuation, of the interannual
829 variation by means of the CV and the calculation of non-standardized anomalies can improve
830 this method.

831 The application of non-standardized anomaly analysis allows us to quantify the critical issues
832 and therefore to determine the "real" potential critical cases. The GWL_AN furnishes the
833 deviation (positive or negative) measured in metres of the GWL from the reference GWL and
834 allows us to examine the nature of the trends, enabling the determination of the dry and wet
835 years. It is important to have a large reference period and to maintain this period for
836 calculating future anomalies. Because the assessment of anomalies also depends on the
837 reference period, it is advisable to use the same reference period for the analysis of the other
838 climatic variables that contribute to the changes in the GWL. The evaluation of GWL_AN is
839 easy to apply and makes the extent of the lowering more evident. The GWL_AN analysis
840 allows us to quantify the critical issues and therefore to determine the "real" potential critical
841 cases.

842 **5. CONCLUSIONS**

843 Numerous factors (hydrogeological, meteorological, anthropogenic activities) play a role in
844 GW behaviour and have to be identified from time to time. Monitoring networks and
845 collection of data are an important starting point for analyzing GW behaviour to better
846 manage water resources. The application of different statistical methods to the GWL series
847 allows us to describe the evolution of the GWL, and the spatialization of the results permits
848 to identify areas with a similar hydrodynamic behaviour and resource evolution.

849 The main aims of the study were the comparison of different statistical methods, highlighting
850 their applicability and differences, and the investigation of the spatiotemporal variation in the
851 GWL of shallow aquifers in the Piedmont Plain, with the description of critical situations of
852 GW depletion.

853 This study highlights that the application of a single method for assessing shallow GW
854 resource evolution does not always guarantee a reliable evaluation. For this reason, as an
855 integration of the methods, it is advisable to apply different analysis methods at the same
856 time. Completeness of data and medium to long time series are prerequisites for meaningful
857 analyses, while the use of the same time interval is necessary for comparisons between
858 different monitoring wells and between the results of different statistical analyses.

859 By spatialising the results, it was possible to identify areas characterised by similar GWL
860 behaviour. These influences vary locally in the Piedmont plain and require local assessments
861 to determine the impact of changes in GWL.

862 Knowledge of current and potential future changes in GWL is important, not only because
863 they are indicative of the total amount of water stored in an aquifer but also because they
864 can support the choices of water management and can provide indications of the degree of
865 exploitation of an aquifer. Understanding the mechanisms and factors that regulate GWL
866 fluctuations and evaluating the GWL over time represent the basis for assessing the
867 quantitative status of shallow aquifers.

868 However, it was seen that the application of different methods provides a clearer picture of
869 the quantitative status of the GW resource and simultaneously highlights the need for further
870 investigation of the recharge dynamics that should consider other climatic and anthropogenic
871 variables as well as the local geological/geographical and climatic setting.

872 Future insights will analyse the effects of other natural factors (climatic, e.g., air temperature,
873 evapotranspiration, snowmelt) and anthropogenic variables (extent of withdrawals) with an
874 in-depth analysis of the local hydrogeological and geological characteristics of the aquifers.
875 The impacts of these factors on groundwater recharge are, indeed, among the most
876 important factors to be evaluated because the variations in GWL depend on the net
877 groundwater recharge and discharge, which relies on these parameters/factors.

878 **Credit authorship contribution statement**

879 **Susanna Mancini:** Conceptualisation, Methodology, Formal analysis, Investigation, Data curation,
880 Visualization, Writing – original draft. **Elena Egidio:** Data curation, Writing – original
881 draft. **Domenico Antonio De Luca:** Methodology, Writing – original draft. **Manuela**
882 **Lasagna:** Conceptualisation, Methodology, Formal analysis, Visualization, Writing – original
883 draft, Supervision.

884 **Declaration of competing interest**

885 The authors declare that they have no known competing financial interests or personal relationships
886 that could have appeared to influence the work reported in this paper.

887 **Conflicts of Interest:**

888 The authors declare no conflict of interest.

889 **REFERENCES**

- 890 Abdul Aziz, O.I., Burn, D.H., 2006. Trends and variability in the hydrological regime of the Mackenzie
891 River Basin, *Journal of Hydrology* 319, 282–294
- 892 Acquaotta, F., Fratianni, S., 2013. Analysis on Long Precipitation Series in Piedmont North-West Italy,
893 *American Journal of Climate Change* 2, 14-24. <http://dx.doi.org/10.4236/ajcc.2013.21002>
- 894 Acquaotta, F., Fratianni, S., Terzago, S., Faletto, M., Prola, M.C., 2013. La neve sulle Alpi Piemontesi:
895 Quadro conoscitivo aggiornato al cinquantennio 1961-2010. Grafica Reventino Srl, 1-97.
896 <https://www.arpa.piemonte.it/pubblicazioni-2/pubblicazioni-anno-2013/arpa-neve-capp1e2.pdf>

897 Allocca, V., Celico, P., 2008. Scenari idrodinamici nella piana ad Oriente di Napoli (Italia), nell'ultimo
898 secolo: cause e problematiche idrogeologiche connesse. *Giornale di Geologia Applicata* 9, 175-198.

899 Amogne, A., Simane, B., Ali Hassen, A., Bantider, A., 2018. Variability and time series trend analysis of
900 rainfall and temperature in northcentral Ethiopia: A case study in Woleka sub-basin. *Weather and
901 Climate Extremes*, 19, 29-41.

902 Apaydin, A., 2009. Response of groundwater to climate variation: fluctuations of groundwater level
903 and well yields in the Halacli aquifer Cankiri, Turkey. *Environ. Monit. Assess.* 2009,
904 <https://doi:10.1007/s10661-009-0976-8>

905 Arora, M., Goel, N.K., Singh, P., 2005. Evaluation of temperature trends over India. *Hydrological
906 Sciences Journal* 50(1): 81–93.

907 Asoka, A., Gleeson, T., Wada, Y., Mishra, V., 2017. Relative contribution of monsoon precipitation
908 and pumping to changes in groundwater storage in India, *Nature Geoscience* 10, p.109–117.

909 ARPA, 2010. ARPA Piemonte. Climate and climate indicators of Piedmont.
910 http://rsaonline.arpa.piemonte.it/meteoclima50/clima_ed_indicatori.htm (accessed 4 November 2021).

911 ARPA, 2016. ARPA Piemonte. Confronti storici – analisi lungo periodo.
912 <https://www.arpa.piemonte.it/rischinaturali/tematismi/clima/confronti-storici/analisi-lungo.html>
913 (accessed 4 November 2021).

914 ARPA, 2018. Il Clima in Piemonte nel 2017.
915 [https://www.arpa.piemonte.it/rischinaturali/tematismi/clima/rapporti-di-](https://www.arpa.piemonte.it/rischinaturali/tematismi/clima/rapporti-di-analisi/annuale_pdf/anno_2017.pdf)
916 [analisi/annuale_pdf/anno_2017.pdf](https://www.arpa.piemonte.it/rischinaturali/tematismi/clima/rapporti-di-analisi/annuale_pdf/anno_2017.pdf) (accessed 4 November 2021).

917 Baronetti, A., Acquaotta, F., Fratianni, S., 2018. Rainfall variability from a dense rain gauge network in
918 North-West Italy. *Climate Research* 75,3,201-213. <https://doi.org/10.3354/cr01517>

919 Bastiancich, L., Lasagna, M., Mancini, S., Falco, M., De Luca, D.A., 2021. Temperature and discharge
920 variations in natural mineral water springs due to climate variability: a case study in the Piedmont Alps
921 (NW Italy). *Environ Geochem Health*. <https://doi.org/10.1007/s10653-021-00864-8>

922 Beaulieu, C., Chen, J., Sarmiento, J.L., 2012. Change-point analysis as a tool to detect abrupt climate
923 variations. *Philosophical Transactions of the Royal Society A*, 370.

924 Beretta, G.P., Avanzini, M., Pagotto, A., 2004. Managing groundwater rise: Experimental results and
925 modelling of water pumping from a quarry lake in Milan urban area (Italy). *Environ Geol* 45, 600-608.

926 Biancotti, A., Bellardone, G., Bovo, S., Cagnazzi, B., Giacomelli, L., Marchisio, C., 1998. Distribuzione
927 regionale di piogge e temperature. *Collana Studi Climatologici in Piemonte*, vol.1, Regione Piemonte,
928 pp. 80.

929 Birsan, M.V., Molnar, P., Burlando, P., Pfaundler, M., 2005. Streamflow trends in Switzerland. *Journal
930 of Hydrology* 314, 312–329

931 Bove, A., Casaccio, D., Destefanis, E., De Luca, D.A., Lasagna, M., Masciocco, L., Ossella, L., Tonussi, M.,
932 2005. *Idrogeologia della pianura piemontese*, Regione Piemonte. Mariogros Industrie Grafiche S.p.A,
933 Torino

934 Braca, G., Bussettini, M., Lastoria, B., Mariani, S., 2013. Anabasi – analisi statistica di base delle serie
935 storiche di dati idrologici – macro a supporto delle linee guida Ispra – manuale d'uso. In: *Linee guida
936 per l'analisi statistica di base delle serie storiche di dati idrologici*. ISPRA, manuali e linee guida n.84/13,
937 Roma, 2013. https://www.isprambiente.gov.it/pre_meteo/idro/ANABASI_ISPRA.html (accessed on
938 02 may 2022)

939 Burn, D.H., Elnur, H.M.A., 2002. Detection of hydrologic trend and variability, *Journal of*
940 *Hydrology*, 255, 107-122

941 Caloiero, T., Coscarelli, R., Ferrari, E. and Mancini, M., 2011. Trend detection of annual and seasonal
942 rainfall in Calabria Southern Italy, *International Journal of Climatology* 311, 44-56.

943 Castagna, S.E.D., De Luca, D.A., Lasagna, M., 2015. Eutrophication of Piedmont quarry lakes north-
944 western Italy: hydrogeological factors, evaluation of trophic levels and management strategies. *J. Env.*
945 *Assmt. Pol. Mgmt* 17:4, 1550036, 21 pp. <https://doi.org/10.1142/S1464333215500362>

946 Costa, M., Gonçalves, M.P., Texeira, L., 2016. Change-point detection in environmental time series
947 based on the informational approach. *Electronic Journal and Applied Statistical Analysis* 92, 267-296.
948 <https://doi.org/10.1285/i20705948v9n2p267>

949 Cuthbert, M.O., Acworth, R., Andersen, M., Larsen, J., McCallum, A., Rau, G.C., Tellam, J., 2015.
950 Understanding and Quantifying Focused, Indirect groundwater Recharge from Ephemeral Streams
951 using Water Table Fluctuations, *Water Resources Research*. Available online at:
952 <http://dx.doi.org/10.1002/2015WR017503> (Accessed 24 November 2021).

953 De Luca, D.A., Falco, F., Falco, M., Lasagna, M., 2005. Studio della variazione del livello piezometrico
954 della falda superficiale nella pianura vercellese (Piemonte). *Giornale di geologia applicata* 2, 387-392.

955 De Luca, D.A., Lasagna, M., Debernardi, L., 2020. Hydrogeology of the western Po Plain Piedmont, NW
956 Italy. *Journal of Maps* 16:2, 265-273. <https://doi.org/10.1080/17445647.2020.1738280>

957 De Luca, D.A., Lasagna, M., Mancini, S. 2019. Strategies for deep aquifers protection at local and
958 regional scale: the Piedmont region example. *GEAM Geingegneria Ambientale e Mineraria* LVI, n. 1,
959 24-29.

960 Döll, P., Fiedler, K., 2008. Global-scale modeling of groundwater recharge, *Hydrol. Earth Syst. Sci.*, 12,
961 863–885. <https://doi.org/10.5194/hess-12-863-2008>

962 Döll, P., Hoffmann-Dobrev, H., Portmann, F.T., Siebert, S., Eicker, A., Rodell, M., Strassberg, G.,
963 Scanlon, B.R., 2012. Impact of water withdrawals from groundwater and surface water on continental
964 water storage variations. *J. Geodyn.* 59–60, 143–156. <https://doi.org/10.1016/j.jog.2011.05.001>

965 Ducci, D., Polemio, M., 2018. Quantitative Impact of Climate Variations on Groundwater in Southern
966 Italy. In: Calvache, M., Duque, C., Pulido-Velazquez, D. (eds) *Groundwater and Global Change in the*
967 *Western Mediterranean Area*. Environmental Earth Sciences. Springer, Cham.
968 https://doi.org/10.1007/978-3-319-69356-9_12

969 EEA, 2018. European Environment Agency (EEA). European waters. Assessment of status and
970 pressures. EEA Report No 7/2018 <https://www.eea.europa.eu/publications/state-of-water>

971 EPA, 2016. ProUCL Software. Statistical Software ProUCL 5.1.00 for Environmental Applications for
972 Data Sets with and without Nondetect Observations. [https://www.epa.gov/land-research/proucl-](https://www.epa.gov/land-research/proucl-software)
973 [software](https://www.epa.gov/land-research/proucl-software) (accessed on 2 may 2022).

974 Fatichi, S., Ivanov, V.Yu., Caporali, E., 2012. Investigating Interannual Variability of Precipitation at the
975 Global Scale: Is There a Connection with Seasonality? *Journal of Climate*, 25, 5512-5523.
976 <https://doi.org/10.1175/JCLI-D-11-00356.1>

977 Helsel, D.R., Hirsch, R.M., Ryberg, K.R., Archfield, S.A., Gilroy, E.J., 2020, *Statistical methods in water*
978 *resources: U.S. Geological Survey Techniques and Methods*, book 4, chap. A3, 458 p.,
979 <https://doi.org/10.3133/tm4a3>

980 Hirsch, R. M., Slack, J. R., Smith, R. A., 1982. Techniques of trend analysis for monthly water quality
981 data. *Water Resources Research*, 181, 107–121

- 982 IAH, 2016. Global Change & groundwater. Strategic Overview Series. [https://iah.org/wp-](https://iah.org/wp-content/uploads/2016/07/IAH-Global-Change-groundwater-14-June-2016.pdf)
983 [content/uploads/2016/07/IAH-Global-Change-groundwater-14-June-2016.pdf](https://iah.org/wp-content/uploads/2016/07/IAH-Global-Change-groundwater-14-June-2016.pdf)
- 984 IPCC, 2022: Climate Change 2022: Impacts, Adaptation, and Vulnerability. Contribution of Working
985 Group II to the Sixth Assessment Report of the Intergovernmental Panel on Climate Change [H.-O.
986 Pörtner, D.C. Roberts, M. Tignor, E.S. Poloczanska, K. Mintenbeck, A. Alegría, M. Craig, S. Langsdorf, S.
987 Löschke, V. Möller, A. Okem, B. Rama (eds.)]. Cambridge University Press.
- 988
989 ISPRA, 2017. Criteri tecnici per l'analisi dello stato quantitativo e il monitoraggio dei corpi idrici
990 sotterranei. Manuali e Linee Guida, Delibera del Consiglio SNPA del 15/05/2017- 8/2017
- 991 Kawamura, A., Bui, D.D., Tong, T.N., Amaguchi, H., Nakagawa, N., 2011. Trend detection in
992 groundwater levels of Holocene unconfined aquifer in Hanoi, Vietnam, by non parametric approaches.
993 <https://doi.org/10.1061/4117341494>
- 994 Kendall, M.G., 1955. Rank Correlation Measures. Charles Griffin, London, 202 pp.
- 995 Kiley, G., 1999. Climate change in Ireland from precipitation and streamflow observations. *Adv. Water*
996 *Resources* 23, 141-151.
- 997 Krishan, G., Chandniha, S. K., Lohani, A. K., 2015. Rainfall Trend Analysis of Punjab, India Using
998 Statistical Non-Parametric Test. *Curr World Environ* 103: 792-800.
999 <http://dx.doi.org/10.12944/CWE.10.3.09>
- 1000 Krogulec, E., Malecki, J.J., Porowoska, D., Wojdalska A., 2020. Assessment of causes and effects of
1001 groundwater level change in an urban area Warsaw, Poland. *Water* 12, 3107.
1002 <https://doi.org/10.3390/w12113107>
- 1003 Kumar, P., Chandniha, S.K., Lohani, A.K., Krishan, G., Nema, A.K., 2018. Trend Analysis of groundwater
1004 Level Using Non-Parametric Tests in Alluvial Aquifers of Uttar Pradesh, India, *Curr. World Environ.* 131,
1005 44-54. <http://dx.doi.org/10.12944/CWE.13.1.05>
- 1006 Lanzante, J. R., 1996. Resistant, robust and non-parametric techniques for the analysis of climate data:
1007 Theory and examples, including applications to historical radiosonde station data, *Int. J. Clim.*, 16,
1008 1197–1226.
- 1009 Lasagna, M., Caviglia, C., De Luca, D.A., 2014. Simulation modeling for groundwater safety in an
1010 overexploitation situation: the Maggiore Valley context (Piedmont, Italy). *Bull. Eng. Geol. Environ.*
1011 73:341–355. [DOI 10.1007/s10064-013-0500-9](https://doi.org/10.1007/s10064-013-0500-9)
- 1012 Lasagna, M., De Luca, D.A., Franchino, E., 2018. Intrinsic groundwater vulnerability assessment: issues,
1013 comparison of different methodologies and correlation with nitrate concentrations in NW Italy.
1014 *Environ. Earth Sci.*, 77, 277. <https://doi.org/10.1007/s12665-018-7452-0>
- 1015 Lasagna, M., Ducci, D., Sellerino, M., Mancini, S., De Luca, D.A., 2020a. Meteorological variability and
1016 groundwater quality: examples in different hydrogeological settings (2020). *Water* 12, 1297.
1017 [doi:10.3390/w12051297](https://doi.org/10.3390/w12051297).
- 1018 Lasagna, M., Mancini, S., De Luca, D.A., Cravero, M., 2019. Piezometric levels in the Piedmont plain
1019 NW Italy: trend and hydrodynamic behaviour of the shallow aquifer. *Rend. Online Soc. Geol. It.* 48:2-
1020 9. <https://doi.org/10.3301/ROL.2019.30>
- 1021 Lasagna, M., Mancini, S., De Luca, D.A., 2020b. Groundwater hydrodynamic behaviours based on
1022 water table levels to identify natural and anthropic controlling factors in the Piedmont Plain Italy,
1023 *Science of the Total Environment* 716, 137051. <https://doi.org/10.1016/j.scitotenv.2020.137051>

- 1024 Liu, J., Cao, G., Zeng, C., 2011. Sustainability of groundwater Resources in the North China Plain,
1025 Sustaining groundwater Resources: A Critical Element in the Global Water Crisis pp.69-87.
1026 http://dx.doi.org/10.1007/978-90-481-3426-7_5
- 1027 Lockwood, J.G., 2001 Abrupt and sudden climatic transitions and fluctuations: a review. *Int. J. Climatol.*
1028 21(9), 1153-1179. <https://doi.org/10.1002/joc.630>
- 1029 Lutz, A., Minyila, S., Saga, B., Diarra, S., Apambire, B., Thomas, J., 2015. Fluctuation of groundwater
1030 Levels and Recharge Patterns in Northern Ghana. *Climate*, 3, 1-15.
1031 <http://dx.doi.org/10.3390/cli3010001>
- 1032 Mann H.B., 1945. Nonparametric tests against trend. *Econometrica*, 13, 245-259.
- 1033 MOE (Ministry of Environment), 2008. Guidance Document for Using the Percentile Method for
1034 Calculating Trigger Levels for Groundwater for the Ontario Low Water Response Plan., Ministry of
1035 Environment, March 2008
- 1036 Ng, G.-H. C., McLaughlin, D., Entekhabi, D., Scanlon, B. R., 2010. Probabilistic analysis of the
1037 effects of climate change on groundwater recharge, *Water Resour. Res.*, 46, W07502,
1038 <https://doi.org/10.1029/2009WR007904>
- 1039 Panda, D. K., Mishra, A., Jena, S. K., James, B. K., Kumar, A., 2007. The influence of drought and
1040 anthropogenic effects on groundwater levels in Orissa, India. *Journal of Hydrology*, 343, 140–
1041 153. <https://doi.org/10.1016/j.jhydrol.2007.06.007>
- 1042 Panda, D., Mishra, A., Kumar, A., 2012. Quantification of trends in groundwater levels of Gujarat in
1043 western India. *Hydrol. Sci. J.* 57, 1325–1336.
- 1044 Pathak, A.A., Dodamani, B.M., 2019. Trend analysis of groundwater levels and assessment of regional
1045 groundwater drought: Ghataprabha River Basin, India *Nat. Resour. Res.* 28, 631.
1046 <https://doi.org/10.1007/s11053-018-9417-0>
- 1047 Patle, G.T., Singh, D.K., Sarangi, A., Anil, R., Khanna, M., Sahoo, R.N., 2015. Time series analysis
1048 of groundwater levels and projection of future trend. *Journal of the Geological Society of India*
1049 852, 232–242.
- 1050 Perotti, L., Carraro, G., Giardino, M., De Luca, D.A., Lasagna, M., 2019. Geodiversity evaluation and
1051 water resources in the Sesia Val Grande UNESCO Geopark (Italy). *Water* 2019, 11, 2102.
1052 [doi:10.3390/w11102102](https://doi.org/10.3390/w11102102)
- 1053 Pettitt, N., 1979. A non parametric approach to the change-point problem. *App. Statist.* 28, n°2.
- 1054 Polemio, M., Casarano, D., 2008. Climate change, drought and groundwater availability in southern
1055 Italy. In: W. Dragoni and B.S. Sukhija Editors, *Climate Change and groundwater*. The Geological Society
1056 Special Publications, 288, pp. 39-51. <https://doi.org/10.1144/SP288.4>
- 1057 Polemio, M., 2016. Monitoring and management of Karstic coastal groundwater in a changing
1058 environment Southern Italy: a review of a regional experience. *Water* 84:1–16
- 1059 Post, R., 2013. Percentile groundwater Indicator Literature Review. Nottawasaga Valley Conservation
1060 Authority 8195 8th Line, Utopia, ON, L0M 1T0 705-424-1479
- 1061 Rai, S. N., Singh, R. N., 1985. Water table fluctuations in response to time varying recharge, in M. Diskin
1062 ed., *Scientific Basis for Water Resources Management*, IAHS Publ. No., 153, 287-294.
- 1063 Reeves, J., Chen, J., Wang, X.L., Lund, R., Lu, Q.Q., 2007. A Review and Comparison of Changepoint
1064 Detection Techniques for Climate Data. *J. Appl. Meteorol. Climatol.* 46, 900–915.

- 1065 Regione Piemonte, 2020. Report 2020 – Analisi clima regionale periodo 1981- 2010 e tendenze negli
 1066 ultimi 60 anni. https://www.regione.piemonte.it/web/sites/default/files/media/documenti/2021-02/analisi_clima_regionale_1981-2010.pdf (accessed 4 November 2021)
 1067
- 1068 Regione Piemonte, 2021a. Idrogeologia – Carta dei complessi idrogeologici.
 1069 https://www.geoportale.piemonte.it/geonetwork/srv/ita/catalog.search#/metadata/r_piemon:6e15300b-d6f1-45a2-a82c-08e2541b1981
 1070
- 1071 Regione Piemonte, 2021b. <http://www.regione.piemonte.it/monitgis/jsp/cartografia/mappa.do>
 1072 (accessed 4 November 2021)
- 1073 Regione Piemonte, 2021c. RAM - Banca dati agrometeorologica | Servizioonline
 1074 <https://servizi.regione.piemonte.it/catalogo/ram-banca-dati-agrometeorologica> (accessed 4
 1075 November 2021)
- 1076 Ribeiro, L., Kretschmer, N., Nascimento, J., Buxo, A., Rötting, T., Soto, G., Señoret, M., Oyarzún, J.,
 1077 Maturana, H., Oyarzún, R., 2015. Evaluating piezometric trends using the MannKendall test on the
 1078 alluvial aquifers of the Elqui River basin, Chile, Hydrological Sciences Journal 60 (10), 1840-1852.
 1079 <https://doi.org/10.1080/02626667.2014.945936>
- 1080 Rusi, S., Chiaudani, A., Palmucci, W., Di Lena, B., 2013. Fluctuations and trends of piezometric levels:
 1081 a case study in Abruzzo. Convegno AIAM
- 1082 Russo, T.A., Lall, U., 2017. Depletion and response of deep groundwater to climate-induced pumping
 1083 variability. Nat. Geosci. 2017, 10, 105–108.
- 1084 Sen, P.K., 1968. Estimates of the regression coefficient based on Kendall's tau. Journal of the American
 1085 Statistical Association 63, 1379–1389.
- 1086 Serrano, A., Mateos, V.L., Garcia, J.A., 1999. Trend analysis of monthly precipitation over the Iberian
 1087 Peninsula for the Period 1921–1995. Physics and Chemistry of the Earth 241–2, 85–90.
- 1088 Soliani, L., 2001. Fondamenti di statistica applicata all'analisi e alla gestione dell'ambiente. Libreria
 1089 medico scientifica, Parma. 1139pp.
- 1090 Stahl, K., Hisdal, H., Hannaford, J., Tallaksen, L.M., van Lanen, H.A.J., Sauquet, E., Demuth, S.,
 1091 Fendekova, M., Jodar, J., 2010. Streamflow trends in Europe: evidence from a dataset of near-natural
 1092 catchments. Hydrol. Earth Syst. Sci. Discuss., 7, 5769–5804
- 1093 Svensson, C., Kundzewicz, W. Z., Maurer, T., 2005. Trend detection in river flow series: 2. Flood and
 1094 low-flow index series, HydrologicalSciences Journal, 50:5.
- 1095 Tabari, H., Nikbakht, J., Some'e, B.S., 2011. Investigation of groundwater level fluctuations in the north
 1096 of Iran, Environmental Earth Sciences, 661, 231-243.
- 1097 Taylor, R.G., Scanlon, B., Döll, P., Rodell, M., Beek, R.V., Wada, Y., Longuevergne, L., Leblanc, M.,
 1098 Famiglietti, J., Edmunds, M., et al., 2013. Ground water and climate change. Nat. Clim. Chang. 2012,
 1099 3, 322–329. <https://doi.org/10.1038/nclimate1744>
- 1100 Tirogo, J., Jost, A., Biao, A., Valdes-Lao, D., Koussoubé, Y., Ribstein, P., 2016 Climate Variability and
 1101 groundwater Response: A Case Study in Burkina Faso West Africa, Water 2016, 8, 171;
 1102 <https://doi.org/10.3390/w8050171>
- 1103 Tomé, A. R., Miranda, P. M. A., 2004. Piecewise linear fitting and trend changing points of climate
 1104 parameters, Geoph. Res. Lett., 31, L02207.
- 1105 Tomozeiu, R., Busuioc, A., Marletto, V., Zinotti, F., Cacciamani, C., 2000. Detection of changes in the
 1106 summer precipitation time series of the region Emilia-Romagna, Italy. Theor. Appl. Climatol. 67,193-
 1107 200.

- 1108 Toreti, A., Desiato, F., Fioravanti, G., Perconti, W., 2010. Seasonal temperatures over Italy and their
1109 relationship with low frequency atmospheric circulation patterns. *J. of Climate Change*, 99, 211-227.
- 1110 Voss, K. A., Famiglietti, J.S., Lo, M., Linage, C., Rodell, M., Swenson, S. C., 2013. Groundwater depletion
1111 in the Middle East from GRACE with implications for transboundary water management in the Tigris-
1112 Euphrates-Western Iran region, *Water Resour. Res.*, 49. <https://doi.org/10.1002/wrcr.20078>
- 1113 Wada, J., van Beek, L.P.H., van Kempten, C., Reckman, J.W.T.M., Vasak, S. and Bierkens, M.P.F., 2010.
1114 Global depletion of groundwater resources. *Geophys. Res. Lett.* 37, I20402
1115 <http://dx.doi.org/10.1029/2010GL044571>
- 1116 Whittemore, D.O., Butler, J.J., Wilson, B.B., 2016. Assessing the major drivers of water-level declines:
1117 new insights into the future of heavily stressed aquifers. *Hydrol. Sci. J.* 61, 134–145
- 1118 WMO, 2007. The Role of Climatological Normals in a Changing Climate WMO/TD-No.1377.
1119 Geneva.Worldwide. *Hydrol. Current Res.* 9: 303.
1120 https://library.wmo.int/index.php?lvl=notice_display&id=16659#.YnahP-hBxPY
- 1121 WMO, 2017. Guidelines on the Calculation of Climate Normals WMO- No. 1203.
1122 https://library.wmo.int/index.php?lvl=notice_display&id=20130#.YnT2UtpBxPY
- 1123 Wu, W.J., Lo, M.H., Wada, J., Famiglietti, J.S., Reager, J.T., Yeh, P.J.F., Ducharne, A., Yang, Z.L., 2020.
1124 Divergent effects of climate change on future groundwater availability in key mid-latitude aquifers.
1125 *Nat Comm.* 11, 3710. <https://doi.org/10.1038/s41467-020-17581-y>
- 1126 Xia, J., Wu, X., Zhan, C., Qiao, Y., Hong, S., Yang, P., Zou, L., 2019. Evaluating the Dynamics of
1127 groundwater Depletion for an Arid Land in the Tarim Basin, *China Water* 11, 186.
1128 <https://doi.org/10.3390/w11020186>
- 1129 Xiong, L., Guo, S., 1994. Trend test and change-point detection for the annual discharge series of the
1130 Yangtze River at the Yichang hydrological station, *Hydrological Sciences Journal*, 49(1), 99-112.
1131 <https://doi.org/10.1623/hysj.49.1.99.53998>
- 1132 Xu, K., Milliman, J.D., Xu, H., 2010. Temporal trend of precipitation and runoff in major Chinese Rivers
1133 since 1951. *Global and Planetary Change* 73(3-4), 219–232.
1134 <https://doi.org/10.1016/j.gloplacha.2010.07.002>
- 1135 Zhang, X., Harvey, K.D., Hogg, W.D., Yuzyk, T. R., 2001. Trends in Canadian streamflow. *Water Resour.*
1136 *Res.* 37, 987–998. <http://dx.doi.org/10.1029/2000WR900357>
- 1137 Zheng C., Liu J., Cao G., Kendy E., Wang H., Jia Y. (2010) - Can China Cope with Its Water Crisis? –
1138 Perspectives from the North China Plain. *Groundwater*, 48(3), 350-354.
- 1139 Zwilling, D., Leete, J., Rongitsch, B., 1989. Understanding groundwater level trend: a key to managing
1140 water use. Division of water, Minnesota department of natural resources.